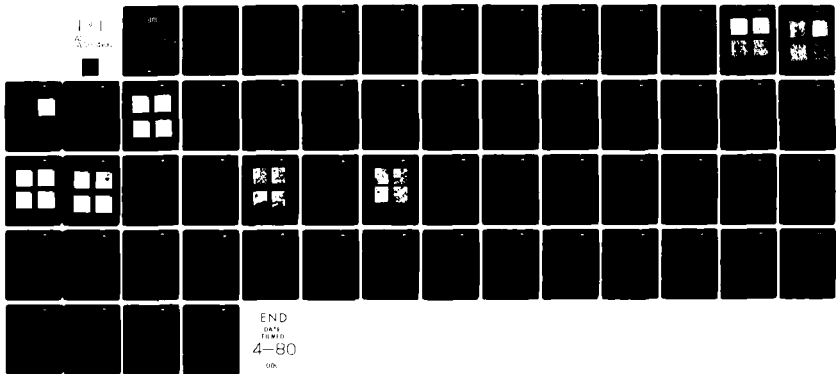


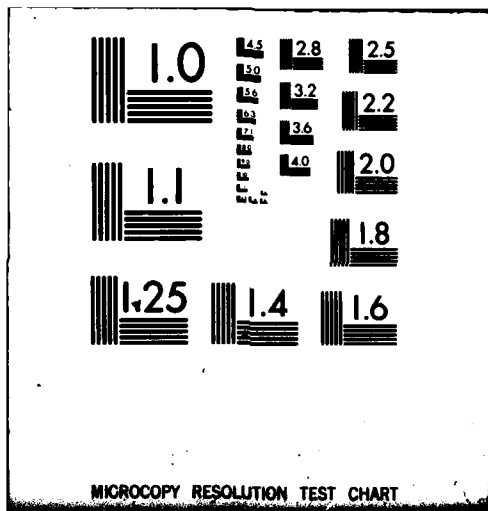
AD-A081 466

ROCKWELL INTERNATIONAL THOUSAND OAKS CA ELECTRONICS--ETC F/G 20/5
LASER ANNEALING OF GAAS. (U)

JAN 80 F H EISEN, J L TANDON, C G KIRKPATRICK MDA903-78-C-0285
ERC41008.11FR NL

UNCLASSIFIED





MICROCOPY RESOLUTION TEST CHART

13

LEVEL

January, 1980

ERC41008.11FR

ADA081466

LASER ANNEALING OF GaAs
Final Technical Report
for period 05/01/78 thru 09/30/79
Contract No. MDA903-78-C-0285
ARPA Order No. 3595
Contract Effective Date 05/01/78
Contract Expiration Date 11/30/79

Rockwell International/Electronics Research Center
Thousand Oaks, California 91360

DTIC
ELECT
MAR 5 1980
C

The views and conclusions contained in this document are those of the author and should not be interpreted as necessarily representing the official policies, either express or implied, of the Defense Advanced Research Projects Agency or the United State Government.

F. H. Eisen

F. H. Eisen
Principal Investigator
Telephone (805) 498-4545

This research was sponsored by the Defense Advanced Research Projects Agency under ARPA Order No. 3671, Contract No. MDA903-78-C-0463, monitored by the Defense Supply Service

This document has been approved for public release and sale; its distribution is unlimited.

DDG FILE COPY



80 2 27 186

UNCLASSIFIED

SECURITY CLASSIFICATION OF THIS PAGE (When Data Entered)

REPORT DOCUMENTATION PAGE		READ INSTRUCTIONS BEFORE COMPLETING FORM
1. REPORT NUMBER	2. GOVT ACCESSION NO.	3. RECIPIENT'S CATALOG NUMBER
4. TITLE (and Subtitle)		5. TYPE OF REPORT & PERIOD COVERED
<p>(C) LASER ANNEALING OF GaAs</p>		Final Technical Report 05/01/78 through 09/30/79
6. AUTHOR(s)		7. PERFORMING ORG. REPORT NUMBER
<p>(10) F. H. Eisen and J. L. Tandon and C.G./Kirkpatrick</p>		<p>(14) ERC41008.11FR</p>
9. PERFORMING ORGANIZATION NAME AND ADDRESS		8. CONTRACT OR GRANT NUMBER(s)
ROCKWELL INTERNATIONAL/ELECTRONICS RESEARCH CENTER 1049 Camino dos Rios Thousand Oaks, California 91360		MDA903-78-C-0285 MDA903-78-C-0463
11. CONTROLLING OFFICE NAME AND ADDRESS		10. PROGRAM ELEMENT, PROJECT, TASK AREA & WORK UNIT NUMBERS
Defense Advanced Research Projects Agency 1400 Wilson Blvd. Arlington, VA 22209		ARPA Order No. 3595
14. MONITORING AGENCY NAME & ADDRESS (if different from Controlling Office)		12. REPORT DATE
Defense Supply Services-Washington Room 1D245, The Pentagon Washington, DC 20310		(11) January 1980
16. DISTRIBUTION STATEMENT (of this Report)		13. NUMBER OF PAGES
<div style="border: 1px solid black; padding: 5px; text-align: center;"> This document has been approved for public release and sale; its distribution is unlimited. </div>		54 (12) 59
		15. SECURITY CLASS. (of this report)
17. DISTRIBUTION STATEMENT (of the abstract entered in Block 20, if different from Report)		15a. DECLASSIFICATION/DOWNGRADING SCHEDULE
<p>(9) Final technical rpt. 5 Jan 78 - 30 Sep 79</p>		UNCLASSIFIED
18. SUPPLEMENTARY NOTES		
19. KEY WORDS (Continue on reverse side if necessary and identify by block number)		
Laser Annealing Electron Beam Annealing Ion Implantation in GaAs GaAs <i>molecular approach</i>		
20. ABSTRACT (Continue on reverse side if necessary and identify by block number)		
<i>lambda approach</i> Irradiations of appropriate energy densities from a pulsed ruby laser ($\lambda = 0.69 \mu\text{m}$, $t_p \leq 15$ or 59 ns) or a pulsed electron beam (energy ≤ 20 keV, $t_p \leq 100$ ns) were found to anneal implanted amorphous layers in GaAs successfully without using an encapsulant. This was confirmed by backscattering/channeling and TEM measurements. Good electrical activation of high dose ($> 10^{15} \text{cm}^{-2}$) implanted donor ions, with peak electron concentrations higher than (10^{19}cm^{-3}), was achieved after both		

DD FORM 1 JAN 73 1473

EDITION OF 1 NOV 65 IS OBSOLETE

UNCLASSIFIED

SECURITY CLASSIFICATION OF THIS PAGE (When Data Entered)

411391

10 to the 19th power cc

JOB

UNCLASSIFIED

SECURITY CLASSIFICATION OF THIS PAGE (When Data Entered)

→ pulsed ruby laser and pulsed electron beam irradiations.

Low dose ($< 10^{13} \text{ cm}^{-2}$) donor ion implanted samples irradiated with ruby laser or electron beam pulses did not show any measurable electrical activity. Possible reasons for this apparent inactivity were explored but the exact reasons are not clear at present.

Au-Ge/Pt ohmic contacts with specific contact resistance as low as $4 \times 10^{-7} \Omega\text{-cm}^2$ were fabricated on n-type GaAs by pulsed electron beam alloying. This value of the specific contact resistance is one of the lowest values reported so far.

10 to the -7th power

↑ $\Omega\text{-cm}^2$

less than 10 to the 13th power cm^{-2}

UNCLASSIFIED

SECURITY CLASSIFICATION OF THIS PAGE (When Data Entered)



Rockwell International
Electronics Research Center

EXTERNAL DISTRIBUTION LIST

Defense Advanced Research Projects Agency
1400 Wilson Boulevard
Arlington, VA 22209
Attention: Program Management
Attention: Dr. R. A. Reynolds
Materials Science Office

Hughes Research Laboratories
3011 Malibu Canyon Road
Malibu, CA 90265
Attention: Dr. C. L. Anderson

Phase-R Corporation
Box G-2
New Durham, NH 03855
Attention: Dr. S. Edward Neister, President

Defense Documentation Center
Cameron Station
Alexandria, VA 22314

Accession For	
NTIS GRA&I	<input checked="" type="checkbox"/>
DDC TAB	<input type="checkbox"/>
Unannounced	<input type="checkbox"/>
Justification	<i>for sample</i>
By	
Distribution/	
Availability Codes	
Dist	Availand/or special
<i>A</i>	



FOREWORD

The research covered in this report was carried out in the Integrated Circuits Section of the Rockwell International Electronics Research Center. The principal contributors were J. L. Tandon, C. G. Kirkpatrick, and F. H. Eisen. Experimental assistance was provided by E. Babcock, P. Fleming, M. Sheets, and E. Walton. The assistance of A. Greenwald, Spire Corporation (electron beam irradiation), C. Robnett, Korad Lasers (laser irradiation), Ilan Golecki, Caltech (backscattering measurements), and D. Sadana, University of California, Berkeley (TEM studies) is gratefully acknowledged.



TABLE OF CONTENTS

	<u>Page</u>
FOREWORD.....	if
TECHNICAL SUMMARY.....	iv
1.0 INTRODUCTION.....	1
2.0 PULSED RUBY LASER ANNEALING OF IMPLANTED GaAs.....	3
2.1 Surface Morphology Studies.....	3
2.1.1 Laser Exposure of Virgin Semi-insulating GaAs.....	3
2.1.2 Laser Exposure of Implanted Semi-insulating GaAs.....	3
2.1.3 Laser Exposure of Implanted and Encapsulated Semi-insulating GaAs.....	7
2.2 Recrystallization of Implanted Amorphous Layer.....	7
2.3 Electrical Measurements.....	11
3.0 PULSED ELECTRON BEAM ANNEALING OF IMPLANTED GaAs.....	19
3.1 Surface Morphology Studies.....	19
3.1.1 Electron Beam Exposure of Low Dose Implanted Semi-insulating GaAs.....	19
3.1.2 Electron Beam Exposure of High Dose Implanted Semi-insulating GaAs.....	19
3.2 Structural and Compositional Studies.....	22
3.3 Electrical Measurements.....	29
4.0 PULSED ELECTRON BEAM ALLOYING OF Au-Ge/Pt OHMIC CONTACTS TO n-TYPE GaAs.....	37
5.0 SUMMARY AND CONCLUSIONS.....	48
6.0 REFERENCES.....	49
7.0 LIST OF PUBLICATIONS.....	51



TECHNICAL SUMMARY

The goals of the program were to investigate the possibility of annealing implanted layers in GaAs using lasers or electron beams, and to characterize the properties of these implanted and annealed layers. This section summarizes the results obtained during the first year of the program.

1. Irradiations of appropriate energy densities from a pulsed ruby laser ($\lambda = 0.69 \mu\text{m}$, $t_p = 15$ or 50 ns) or a pulsed electron beam (energy ≈ 20 keV, $t_p = 100$ ns) were found to anneal implanted amorphous layers in GaAs successfully without using an encapsulant. This was confirmed by backscattering/channeling and TEM measurements.

2. Good electrical activation of high dose ($>10^{15} \text{ cm}^{-2}$) implanted donor ions, with peak electron concentrations higher than 10^{19} cm^{-3} , was achieved after both pulsed ruby laser and pulsed electron beam irradiations.

3. Low dose ($<10^{13} \text{ cm}^{-2}$) donor ion implanted samples irradiated with ruby laser or electron beam pulses did not show any measurable electrical activity. Possible reasons for this apparent inactivity were explored but the exact reasons are not clear at present.

4. Au-Ge/Pt ohmic contacts with specific contact resistance as low as $4 \times 10^{-7} \Omega\text{-cm}^2$ were fabricated on n-type GaAs by pulsed electron beam alloying. This value of the specific contact resistance is one of the lowest values reported so far.



1.0 INTRODUCTION

The desire to fabricate microwave devices/circuits has generated considerable interest over the last few years in the production of controlled, reproducible n-type layers in GaAs by ion implantation.¹⁻⁴ Since dissociation of GaAs can occur at the high temperatures (>700°C) typically required for post-implantation annealing, thermal annealing of implanted GaAs usually has been carried out using an encapsulant (e.g., SiO₂, Si₃N₄, AlN, etc.) to prevent the escape of As. Although the escape of As can be largely prevented, significant outdiffusion of Ga sometimes occurs through the encapsulant during thermal treatment. In addition, adherence of the encapsulant during the annealing, which is a strong function of the technique used to deposit the encapsulant, is sometimes a problem. These aspects of thermal annealing of implanted layers in GaAs make possible alternative approaches to damage removal and electrical activation, such as laser or electron beam annealing ion-implanted GaAs without an encapsulant, attractive. The contract "Laser Annealing of GaAs" was aimed at such an effort. In this final report, major results are summarized. Primarily, a pulsed ruby laser and a pulsed electron beam were primarily explored to anneal implantation damage in GaAs. The properties of the irradiated samples were analyzed by several techniques, including differential Hall effect measurements, backscattering/channeling, optical microscopy, transmission electron microscopy (TEM), secondary ion mass spectrometry (SIMS) and Auger electron spectroscopy (AES).

The observations made on the annealing effects of a pulsed ruby laser on ion-implanted GaAs are described in Section 2. For ion implanted amorphous layers, an energy density threshold was found to exist for recrystallization. Above the threshold, the amorphous layer regrew epitaxially, and below the threshold, the layer became polycrystalline; the grain size increased as the energy density approached the threshold. Good activation (~20%) of high dose (~10¹⁵ cm⁻²) implanted donor ions (Si, Se) was achieved after pulsed ruby laser irradiation. However, the Hall mobilities were poor when compared with capped and thermally annealed samples. Low dose (<10¹³ cm⁻²) donor implanted layers



in semi-implanting GaAs did not show any measurable electrical activity after irradiation.

The results of similar experiments performed on pulsed electron beam annealing of semi-insulating GaAs are discussed in Section 3. An energy density threshold behavior in the electron beam pulse for the recrystallization of amorphous layers was again observed. As observed for ruby laser irradiation, high dose ($>10^{15}$ cm⁻²) implanted donor ions resulted in high activation and the low dose ($<10^{13}$ cm⁻²) donor ion implanted samples again showed insignificant electrical activity.

Several experiments were designed and carried out to investigate the reasons for higher activation of implanted Se in the high dose (10^{15} cm⁻²) and lower activation in the low dose ($<10^{13}$ cm⁻²) implanted and irradiated samples. A pulsed electron beam was used for most of these experiments. The results are discussed in Section 3. Although some insight is provided for the possible mechanisms involved, the exact reasons are still not clear.

In Section 4 some of the more recent experiments conducted on the pulsed electron beam alloying of Au-Ge/Pt ohmic contacts to n-type GaAs are reported. Specific contact resistance as low as 4×10^{-7} Ω -cm² was achieved after pulsed electron beam alloying.

Finally, Section 5 has concluding remarks. Results obtained to date are summarized with some suggestions for future experiments.



2.0 PULSED RUBY LASER ANNEALING OF IMPLANTED GaAs

In this section, effects of a ruby laser pulse ($\lambda = 0.694 \mu\text{m}$, $t_p = 15$ or 50 ns) on implanted GaAs are described and discussed. All samples were irradiated in air.

2.1 Surface Morphology Studies

2.1.1 Laser Exposure of Virgin Semi-insulating GaAs

Wafers of semi-insulating GaAs were exposed in air to ruby laser pulses with various energy densities. Figure 1 shows Nomarski optical photographs of the surfaces after irradiation. Even at 0.72 J/cm^2 (energy density less than the threshold value for annealing implanted GaAs⁵), the exposed area indicated melting in localized regions, which was possibly due to hot spots in the laser. As the energy density was increased, evidence of melting over larger areas was observed (see Fig. 1a-d). Generally, with the ruby laser, resolidification after melting was almost always found to be non-uniform. The spatial energy distribution in the laser spot seemed to be a factor in obtaining exposures that appeared featureless as viewed under the optical microscope magnification.

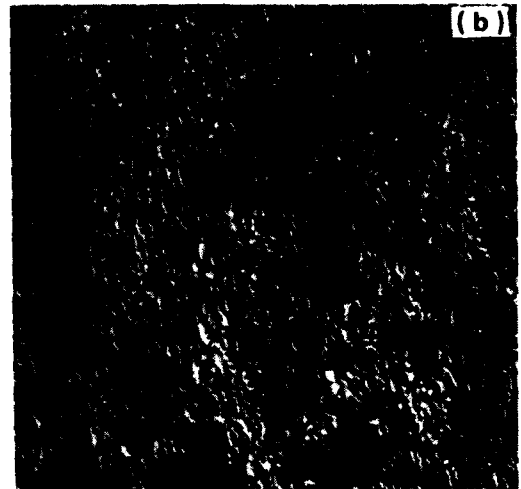
2.1.2 Laser Exposure of Implanted Semi-insulating GaAs

Figure 2 shows photographs of the surfaces of semi-insulating GaAs samples implanted with 10^{15} 300 keV Se^+ ions/cm² and irradiated with laser pulses of various energy densities. Increased melting over larger areas with increasing energy density was again observed. These photographs probably represent the regions with the worst texture when viewed under the microscope. However, the samples were also found to contain regions which were essentially featureless, as evidenced by Fig. 3, where photographs of these samples exposed to the lowest (0.75 J/cm^2) and the highest (1.51 J/cm^2) values of laser energy densities (see Fig. 2) are shown. It should be noted that all samples



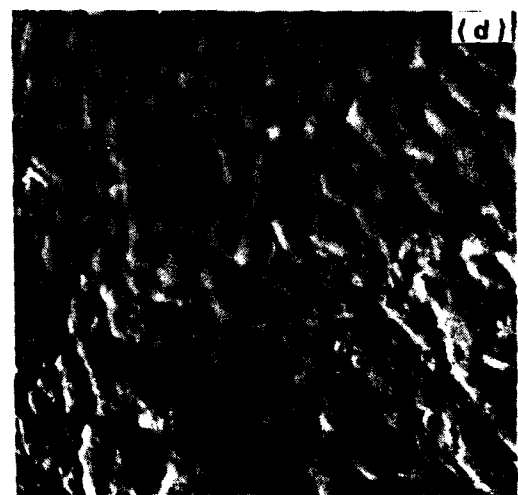
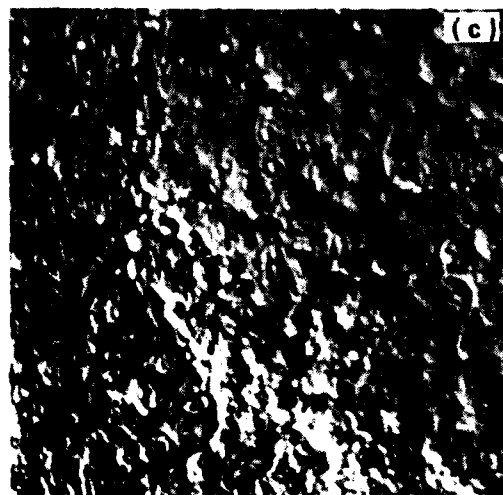
SC79-4279

GaAs



0.72 J/cm²

1.20 J/cm²



1.75 J/cm²

100μm
|-----|

2.01 J/cm²

Fig. 1 Surface morphology of semi-insulating GaAs after irradiation with a ruby laser pulse of energy density: (a) 0.72 J/cm², (b) 1.20 J/cm², (c) 1.75 J/cm² and (d) 2.01 J/cm².



SC79-4280

Se \rightarrow GaAs, R. T., 300 keV, $1 \times 10^{15} \text{ cm}^{-2}$
RUBY LASER ANNEAL, NO ENCAPSULANT

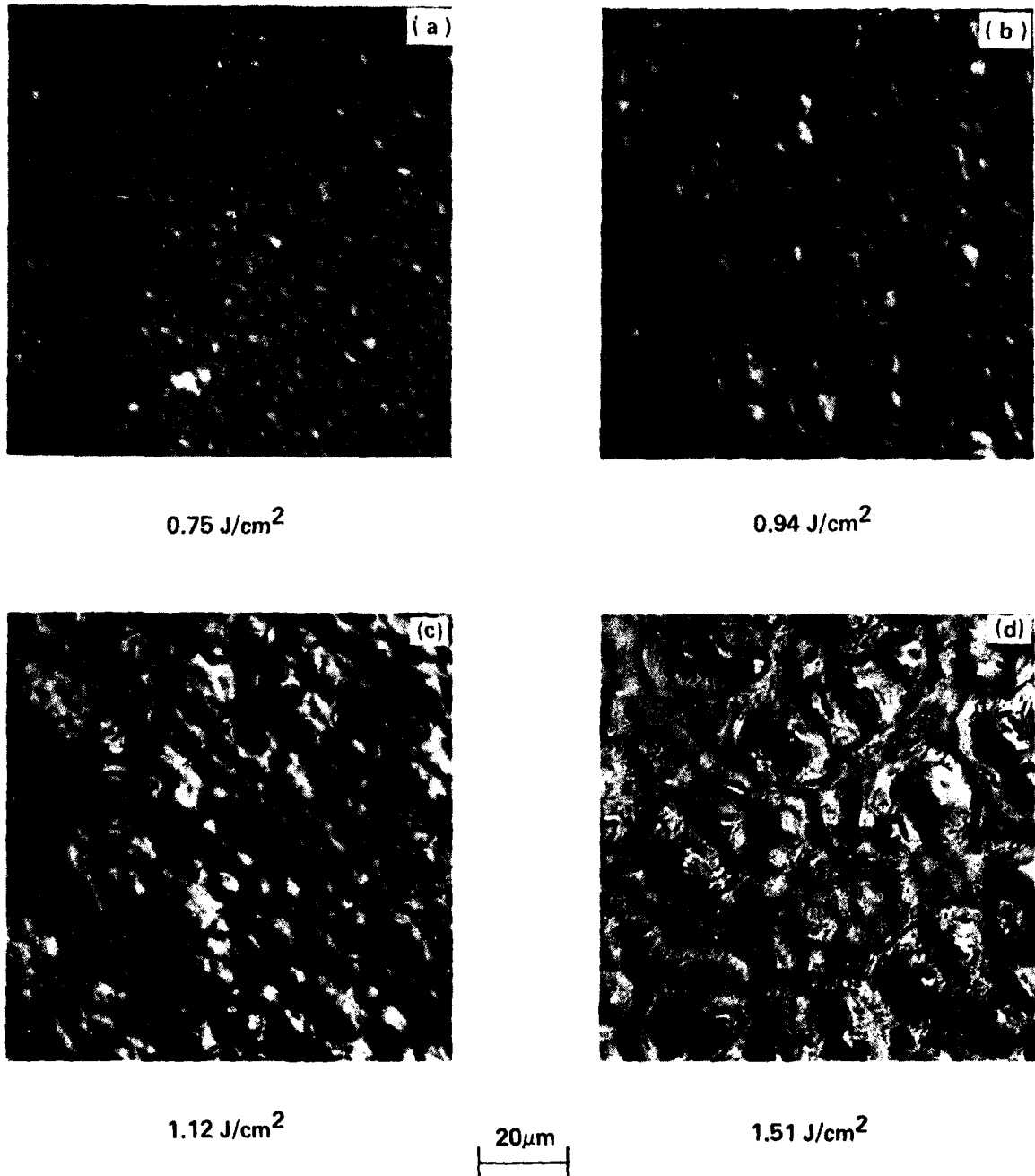


Fig. 2 Surface morphology of implanted (300 keV , $1 \times 10^{15} \text{ Se}^+/\text{cm}^2$ semi-insulating GaAs after irradiation with a ruby laser pulse of energy density: (a) 0.75 J/cm^2 , (b) 0.94 J/cm^2 , (c) 1.12 J/cm^2 , and (d) 1.51 J/cm^2 .



Se → GaAs, R. T., 300keV, $1 \times 10^{15} \text{ cm}^{-2}$ RUBY
LASER ANNEAL, NO ENCAPSULANT

SC79-4281

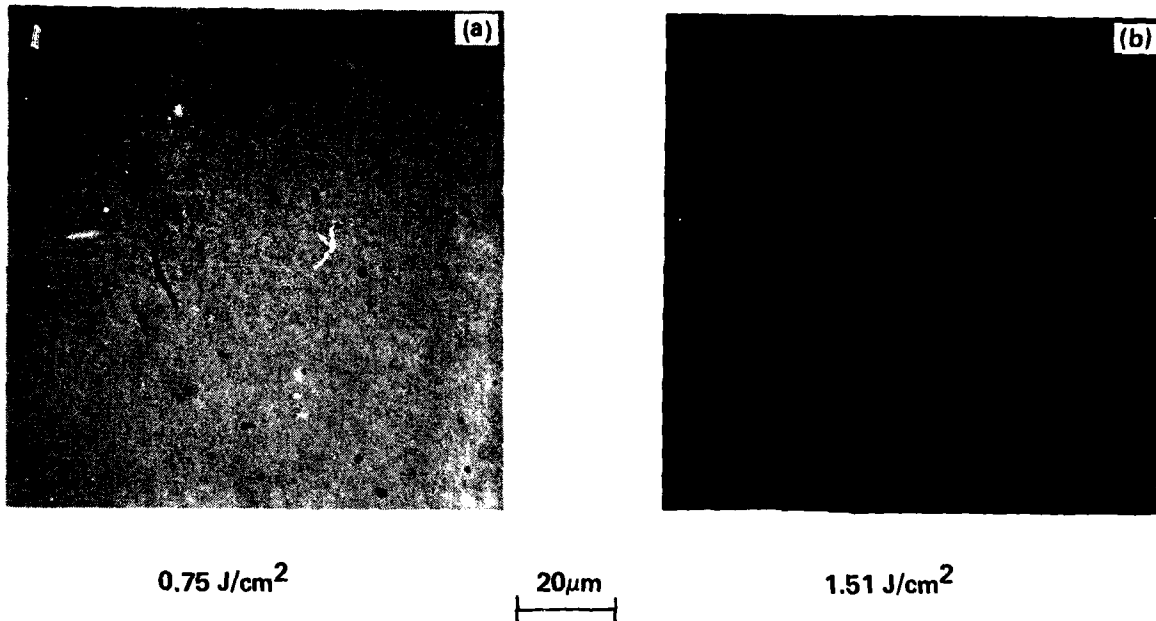


Fig. 3 Surface morphology of selected small uniform regions from the samples shown in Fig. 2(a) and (d).



with surfaces shown as in Fig. 2 were found to possess good electrical activation of the Se ions over areas of dimensions 7 mm x 7 mm employed for measurements.

2.1.3 Laser Exposure of Implanted and Encapsulated Semi-insulating GaAs

Semi-insulating GaAs samples were implanted with 300 keV 10^{15} Se^+ ions/cm² and irradiated with ruby laser pulses after being capped with ~1000Å of reactively sputtered Si_3N_4 films. Figure 4 depicts the surfaces of these samples after irradiation with different energy densities of the laser. It was found that the Si_3N_4 film cracked, presumably due to thermal stresses, when exposed to a laser pulse with energy density as low as 0.59 J/cm². Larger cracks were introduced in the Si_3N_4 film with a laser pulse of higher energy density (Fig. 4b), and with a pulse of energy density >1.3 J/cm², the Si_3N_4 film was completely vaporized from the area exposed to the laser beam (Figs. 4c and d). The samples in Figs. 4c and 4d also indicated melting and resolidification of the GaAs surface beneath. The texture of the surfaces after resolidification, however, appeared to be somewhat finer than the texture of the surfaces of uncoated samples exposed to laser irradiation (compare Fig. 4 with Figs. 1 and 2). Since the Si_3N_4 film cracked or vaporized when the coated samples were irradiated with laser energy densities sufficient for successful annealing, the Si_3N_4 film did not seem to function in protecting the stoichiometry of the GaAs surface as in conventional thermal annealing of implanted GaAs.

2.2 Recrystallization of Implanted Amorphous Layers

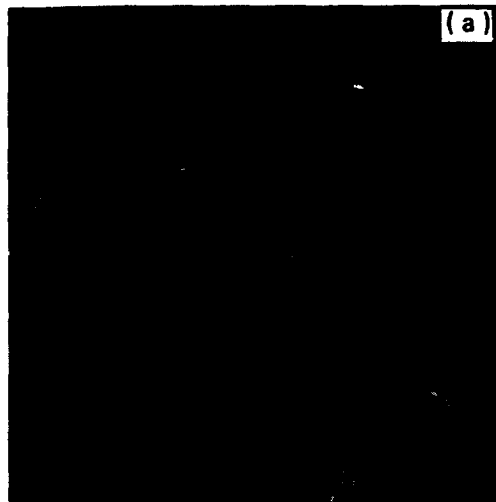
Semi-insulating GaAs wafers of <100> orientation were implanted at room temperature with 400 keV Te to a fluence of about 1×10^{15} cm⁻². This implantation produced an amorphous layer of about 2300Å thickness. To minimize channeling, the ion beam was oriented at an angle of ~10° against the normal to the wafer surface.

The incident laser energy density varied from 0.2 to 2.0 J/cm². Channeling and backscattering spectrometry measurements were performed with



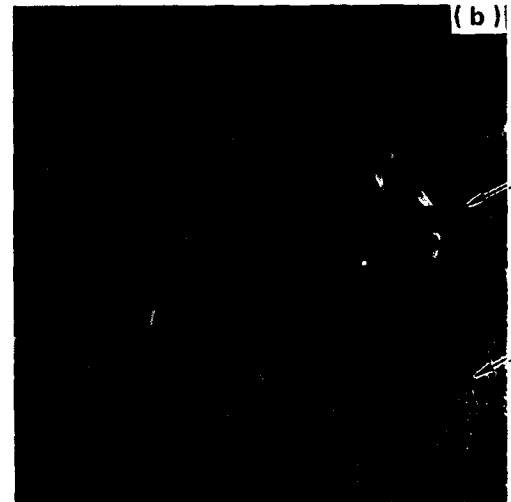
Se → GaAs, R. T., 300 keV, $1 \times 10^{15} \text{ cm}^{-2}$ RUBY
LASER ANNEAL, 1000Å Si_3N_4

SC79-4282



(a)

0.59 J/cm²

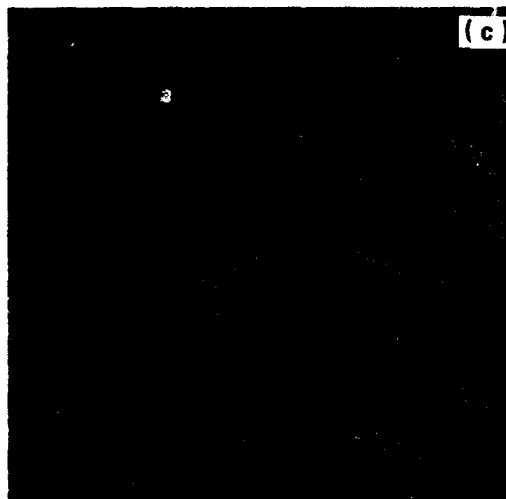


(b)

0.72 J/cm²

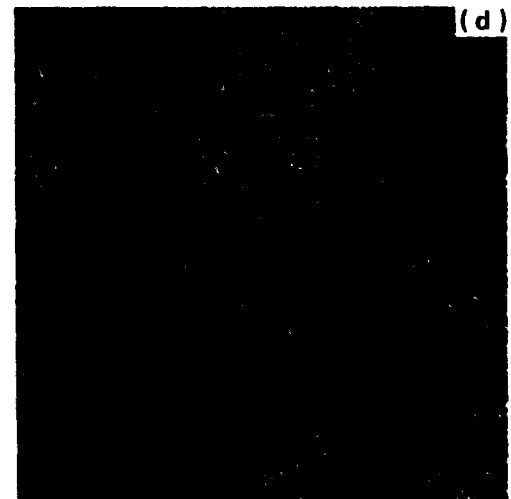
Si_3N_4

EXPOSED
GaAs



(c)

1.3 J/cm²



(d)

1.75 J/cm²

100μm

Fig. 4 Surface morphology of semi-insulating GaAs samples coated with ~1000Å Si_3N_4 film after irradiation with a ruby laser pulse of energy density: (a) 0.59 J/cm², (b) 0.72 J/cm², (c) 1.3 J/cm², and (d) 1.75 J/cm². All samples were implanted with 300 keV, $1 \times 10^{15} \text{ cm}^{-2}$ Si⁺ ions at room temperature prior to Si_3N_4 coating and laser irradiation.



ERC41008.11FR

2.5 MeV $^4\text{He}^+$ to investigate the thickness of the damaged layer and its recovery after laser irradiation. Information on the microstructure of the layer after laser irradiation was obtained by transmission electron microscopy.

Channeling effect measurements indicated that the recovery of the implanted amorphous layer exhibited a threshold with laser beam energy density. This threshold had a value of about 1.0 J/cm^2 . Above the threshold value, the backscattering yield observed with $\langle 100 \rangle$ aligned incidence of the He beam became comparable to that measured on an unimplanted single-crystal wafer, as shown in Fig. 5. A backscattering spectrum taken at random incidence of the He beam showed that the Te implantation destroyed the monocrystalline structure of the wafer over a depth of approximately 2300\AA . This layer was amorphous in structure as was determined by electron diffraction measurements. A ruby laser pulse of 1 J/cm^2 thus transformed the implanted amorphous layer into an epitaxial layer with good crystalline quality. For energy densities below 0.8 J/cm^2 , the yield observed with aligned He beam incidence decreased only by about 50%. No movement of the original amorphous-to-crystal interface was detected. In the range of 1.0 to 1.4 J/cm^2 , beyond threshold, channeling gave the same spectrum, and this spectrum differed little from that of an unimplanted wafer.

TEM measurements indicated that at 0.6 J/cm^2 irradiation, polycrystalline material was formed. At 1.0 J/cm^2 single-crystalline material was formed with stacking faults and with dislocations whose density was about $3 \times 10^5/\text{cm}^2$. At 1.4 J/cm^2 single-crystalline material was formed with dispersed defects of about $3 \times 10^{10}/\text{cm}^2$. These defects were less than 100\AA in size and were located very near the surface as was determined by stereo-micrographs. The physical identity of these defects has yet to be established.

From the difference in the microstructures of the irradiated samples the existence of a threshold energy density was noted. Its value was determined to be near 1.0 J/cm^2 . The size of the grains in polycrystalline layers obtained after laser irradiation below the threshold depended on the energy density of the ruby laser pulse. The average dimension of the grains in the



ERC41008.11FR

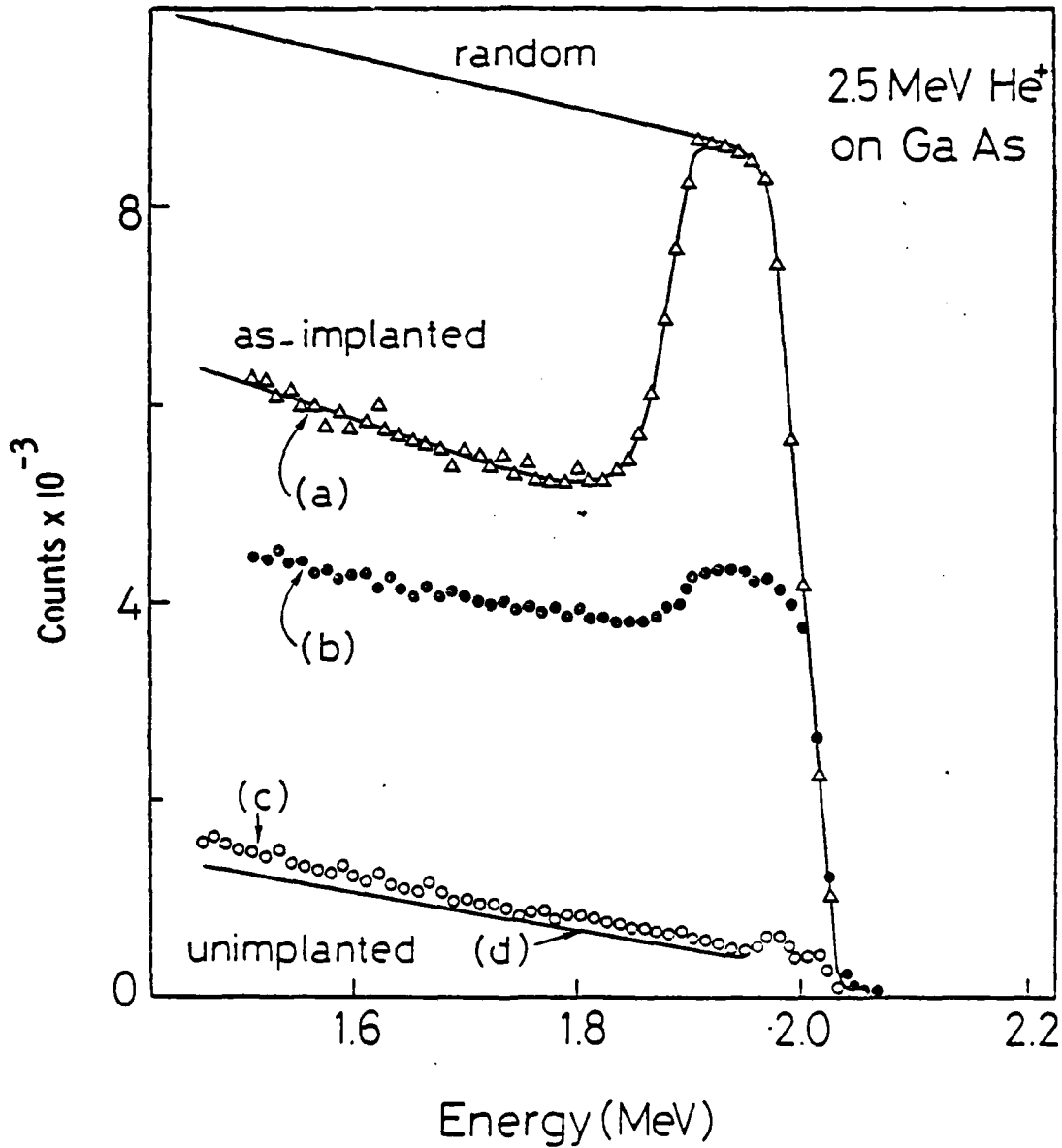


Fig. 5 Backscattering spectra of 2.5 MeV He⁺ ions incident in a random direction and in <100> direction of GaAs samples implanted with 400 keV Te (10^{15} cm^{-2}), after laser irradiation of energy (a) 0.2 to 0.8 J/cm², (b) 0.9 J/cm², (c) 1.0 to 1.4 J/cm². The curve (d) is obtained from unimplanted <100> GaAs sample.



polycrystalline layers was determined from TEM measurements. The average grain size increased with increasing energy density of the laser irradiation. These results are summarized in Fig. 6. The bars represent the spread in the distribution of the grain diameter. The average grain size had a range from 400 to 1100Å on going from 0.2 to 0.9 J/cm². Near the threshold (~1.0 J/cm²) the lateral nonuniformities of the ruby laser spot became crucial in determining the structural configuration of the irradiated layer.

The existence of a threshold energy separating films of polycrystalline and single-crystalline structure, depending on the energy density of the laser irradiation as well as the dependence of grain size on energy density below threshold observed here for GaAs was analogous to the results found with Si. Therefore, the results can be interpreted in the same fashion, as was initially proposed by E. I. Shtyrkov et al.⁶. Above threshold, the energy deposited by the laser beam sufficed to melt a layer of GaAs which exceeded the depth of the amorphous implanted layer. Below threshold, the molten zone never reached the underlying single-crystalline substrate and thus did not regrow epitaxially.

2.3 Electrical Measurements

Several semi-insulating <100> wafers of Cr-doped GaAs were implanted with 300 keV Se⁺ ions at room temperature. The dose range selected was $3 \times 10^{12} - 1 \times 10^{15}$ Se⁺ ions/cm². To minimize channeling during implantation, the ion beam was oriented at an angle of about 7° to the normal to the wafer surface. Laser annealing was accomplished in air by a Q-switched ruby laser pulse. The incident energy densities employed were in the range 0.8 - 1.2J/cm² in order to conform to the threshold annealing values observed in GaAs.⁵

Table I summarizes typical results of Hall-effect measurements made on some of the samples implanted with 10^{15} Se⁺ ions/cm² and subsequently annealed thermally or by a laser pulse. The measurements were made after etching Van der Pauw type mesas provided with Au-Ge/Pt ohmic contacts.⁴ Better activation of Se⁺ ions was achieved in the samples annealed by the

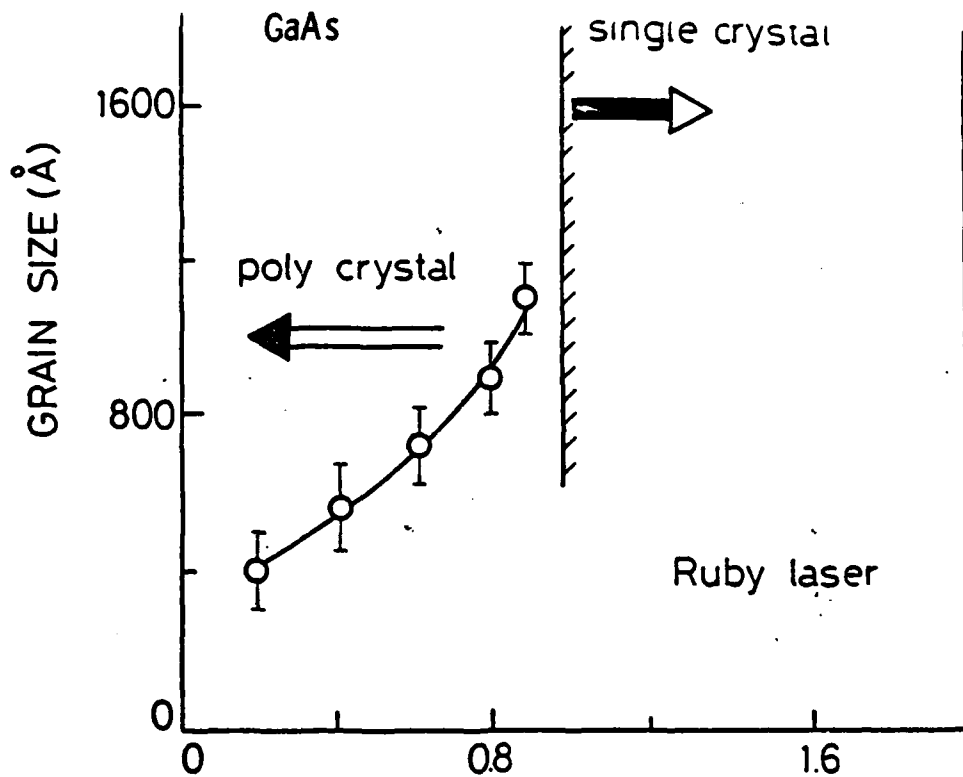


Fig. 6 Average grain size obtained from TEM micrographs of the polycrystalline GaAs layer formed by transient annealing with a ruby laser pulse of varying energy density. Prior to the laser irradiation, the $\langle 100 \rangle$ GaAs substrate had been implanted with 400 keV Te at room temperature to a dose of $1 \times 10^{15} \text{ cm}^{-2}$. The bars represent the spread in the diameter of the grains.



ERC41008.11FR

laser, with or without a Si_3N_4 encapsulant, when compared to the sample annealed thermally. The measured effective sheet electron concentration (N_e) was significantly higher in the laser annealed samples compared to the corresponding value in the thermally annealed sample, even though the thermally annealed sample was implanted at 350°C . This result could be due in part to the incorporation of Se atoms on substitutional sites in the GaAs crystal after laser irradiation being higher than after thermal annealing. It should be noted, however, that all substitutional impurity atoms might not be electrically active in the GaAs crystal, as experiments conducted on bulk grown Te-doped GaAs and Te implanted GaAs^{7,8} have indicated. Considering this possibility, significantly lower concentrations of compensating defects might also account for the higher values of N_e measured in the pulse annealed samples, when compared to the thermally annealed sample. The relatively low values of effective mobility (μ_e) found in the laser annealed samples (that is

Table I

Comparison of the Sheet-Resistance (ρ_s), the Effective Sheet Electron Concentration (N_e), and the Effective Mobility (μ_e) for Semi-Insulating GaAs Implanted with $300 \text{ keV } 1 \times 10^{15} \text{ Se}^+$ ions/ cm^2 and Annealed Thermally, or by a Ruby Laser Pulse

	Thermal (350°C) AlN- 900°C - $10'$ - H_2	Ruby Laser (R.T.) $1\text{J}/\text{cm}^2$ Si_3N_4 (1000A)	$1\text{J}/\text{cm}^2$ No Cap
ρ_s (Ω/\square)	130.5	143.2	130.3
N_e (cm^{-2})	3×10^{13}	1.9×10^{14}	1.4×10^{14}
μ_e (cm^2/vs)	1720	225	334



ERC41008.11FR

low in comparison to the thermally annealed sample) might be partially due to the higher density of ionized impurity centers in the laser annealed samples. Also, the laser annealed samples might contain certain residual defects or electron scattering centers which might contribute toward lowering the mobility. From the data in Table I, it was noted that satisfactory annealing of implanted GaAs could be accomplished using laser irradiation with or without an encapsulant.

It was observed that, with incident irradiation energy densities similar to those used to anneal the samples implanted with 10^{15} Se^+ ions/ cm^2 , no measurable electrical activity could be detected in the laser irradiated samples implanted with $< 10^{14}$ Se^+ ions/ cm^2 . This result indicated that low dose implants ($< 10^{14}/\text{cm}^2$) did not anneal as well as high dose implants ($10^{15}/\text{cm}^2$) when similar ranges of incident energy densities of laser pulse irradiation were employed.

Figure 7 shows the depth profiles of the electron concentration (N) and of the electron mobility (μ) for the two laser annealed samples (see Table I). These profiles were obtained by successive stripping of surface layers combined with Hall-effect and resistivity measurements.⁴ The LSS profile, calculated using a Gaussian approximation,⁹ is also shown for comparison. The measured profiles showed no correlation to the LSS profile in shape and they appeared to be deeper than the range predicted by the LSS theory. This result was, however, not too surprising, as deeper profiles were also found in thermally annealed samples implanted with similar doses.⁽¹⁾ The evidence of higher activation measured in the sample which was laser annealed with Si_3N_4 encapsulation, when compared to the sample annealed without an encapsulant, was not clear. Nevertheless, electron concentrations in excess of $10^{19}/\text{cm}^3$ were measured in both of the laser annealed samples, which were at least a factor of two higher than the concentrations measured in capped and thermally annealed samples⁽¹⁾ implanted with similar doses and energy of Se^+ ions. The mobility profiles in Fig. 7 showed that the mobility was significantly lower in both of the laser annealed samples when compared to the values for bulk GaAs¹⁰ for a similar range of peak electron concentrations.



ERC41008.11FR

SC78-3035

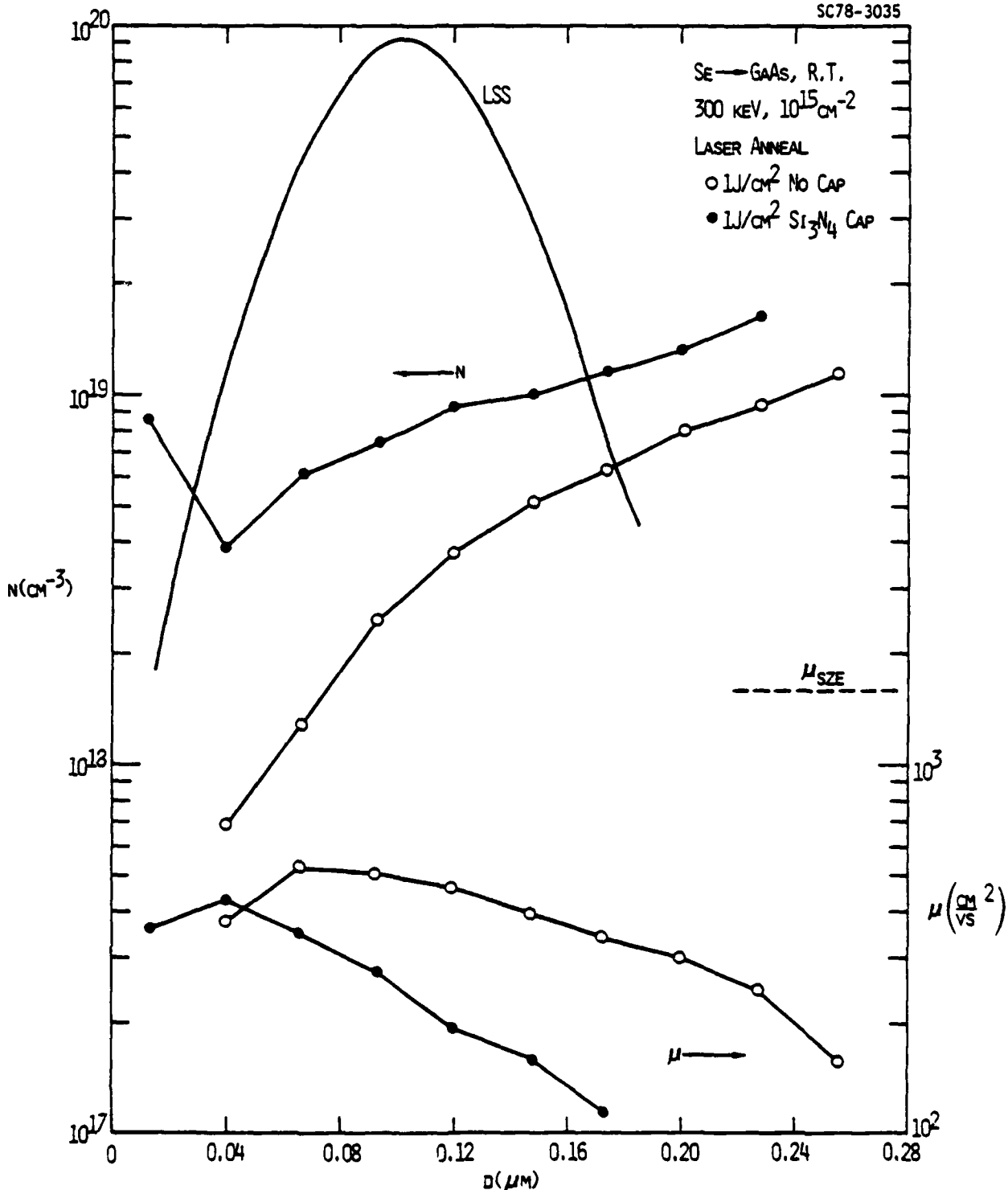


Fig. 7 Depth profiles of the electron concentration (N) and of the electron mobility (μ) measured in the two laser annealed samples (Table I), one annealed with and the other without a Si₃N₄ encapsulant. The incident energy densities employed were the same in the two samples.



ERC41008.11FR

Further experiments were carried out to study the effect of implant temperature on the activation of Se. Semi-insulating $\langle 100 \rangle$ GaAs wafers were implanted with 300 keV Se^+ ions at 296K or 125K to a dose of $1 \times 10^{15} \text{ cm}^{-2}$. Although implantations at both temperatures produced an amorphous layer, the amorphous layer for the 125K implants was expected to be thicker. After implantation, the unencapsulated samples were irradiated with ruby laser pulses of different energy densities. Measurements of sheet electron concentration (N_s), effective mobility (μ_e) and sheet resistance (ρ_s) were then made on these samples. In Fig. 8 these measurements are summarized. Samples implanted at 125K appeared to require higher laser pulse energy densities for about equal values of measured sheet electron concentration, when compared with the samples implanted at 296K. It was interesting to note that the sample implanted at 125K and annealed with a 1.5 J/cm^2 laser pulse not only had high activation ($N_s = 1.4 \times 10^{14} \text{ cm}^{-2}$) but also a high value of μ_e ($1.6 \times 10^3 \frac{\text{cm}^2}{\text{Vs}}$). Correspondingly, this sample had a very low value of sheet resistance ($18 \Omega/\square$).

From a comparison of the electrical measurements made on samples implanted with 300 keV, 10^{15} Se^+ ions/cm² at 296K or 125K, and annealed with various energy densities of the ruby laser, it was revealed that the thickness of the amorphous layer might play a significant role. For best annealing conditions, the parameters of the beams should be adjusted according to the implantation conditions to optimize the melt depth and the time duration for which the layer remains molten.

Several samples implanted with lower doses ($< 10^{14} \text{ cm}^{-2}$) of Se^+ at 296K or 125K were also irradiated with laser pulses possessing similar values of energy densities and beam parameters. No significant differences in the measured electrical activity were found between the samples implanted at the two temperatures. All samples showed poor or non-measurable electrical activity. Since the implantation dose threshold for the amorphization of GaAs was expected to be different for the two implantations, lower for the 125K case, it appeared that the formation of an amorphous layer might not be



ERC41008.11FR

SC79-5006

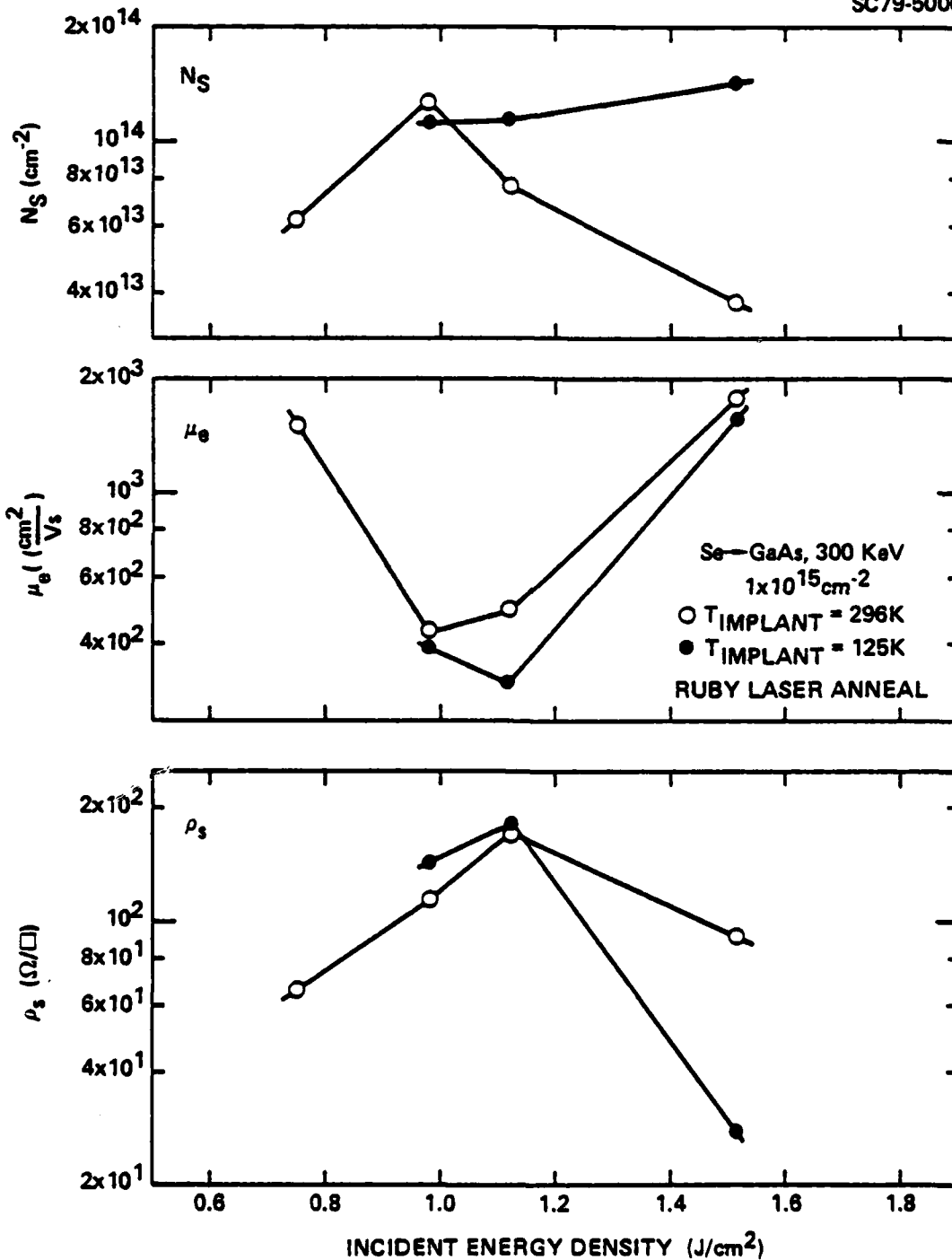


Fig. 8 Sheet electron concentration (N_s), effective mobility (μ_e) and sheet resistance (ρ_s) measured in the ruby laser annealed GaAs samples vs the incident energy density of the laser pulse. The samples were implanted with 300 keV, $1 \times 10^{15} \text{ Se}^+/\text{cm}^2$ at 296°K (\circ) or at 125°K (\bullet) prior to laser irradiation.



ERC41008.11FR

necessary for the activation of Se in the implanted layers irradiated with ruby laser pulses with the parameters chosen.



3.0 PULSED ELECTRON BEAM ANNEALING OF IMPLANTED GaAs

In this section, effects of single electron beam, pulses (mean electron energy = 20 keV, $t_p = 100$ ns) on implanted GaAs are described and discussed.

3.1 Surface Morphology Studies

3.1.1 Electron Beam Exposure of Low Dose Implanted Semi-insulating GaAs

In Fig. 9, the surfaces of semi-insulating GaAs samples implanted with 3×10^{12} 300 keV Se^+ ions/cm² and irradiated with various values of electron beam energy densities are compared with the surface of the as-implanted sample. The electron beam exposed area appeared to be much more uniform compared to the laser exposed areas (compare Fig. 9 with Figs. 1 and 2). The areas shown in Fig. 9 should be considered as representative of typical surface morphology over the electron beam irradiated spot. At an electron beam energy density of 0.67 J/cm² (Fig. 9c), considerable pitting of the surface is observed which was followed by cracking of the surface at a higher energy density of 1.05 J/cm² (Fig. 9d). The cracks were probably caused by thermal stresses and seemed to occur along well defined planes. Similar cracks have also been observed in Si samples irradiated with electron beam pulses of high energy densities.¹¹

3.1.2 Electron Beam Exposure of High Dose Implanted Layers in Semi-insulating GaAs

Semi-insulating GaAs wafers were implanted with 1×10^{15} 300 keV Kr^+ ions/cm² at room temperature. Figure 10 shows the surface morphology of these samples after irradiation with different energy densities of electron beam pulses. For comparison, the surface of the as-implanted sample is also shown (Fig. 10a). It was interesting to note that the energy density threshold for the surface damage by the electron beam pulse in this set of samples was different from the samples implanted with a low dose (3×10^{12} /cm²) of Se



Se→GaAs, R. T., 300 keV, $3 \times 10^{12} \text{ cm}^{-2}$ ELECTRON
BEAM ANNEAL, NO ENCAPSULANT

SC79-4283

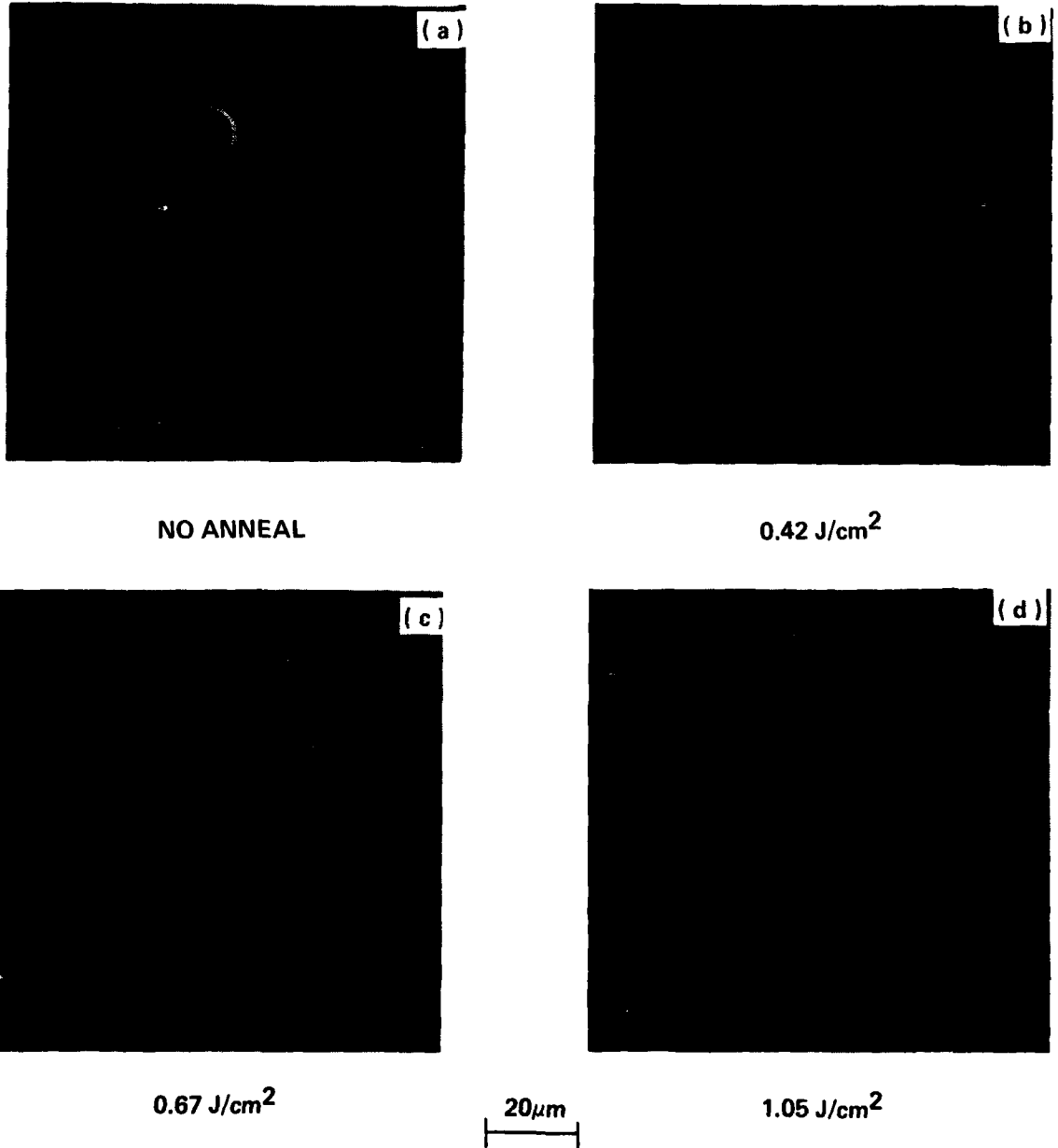
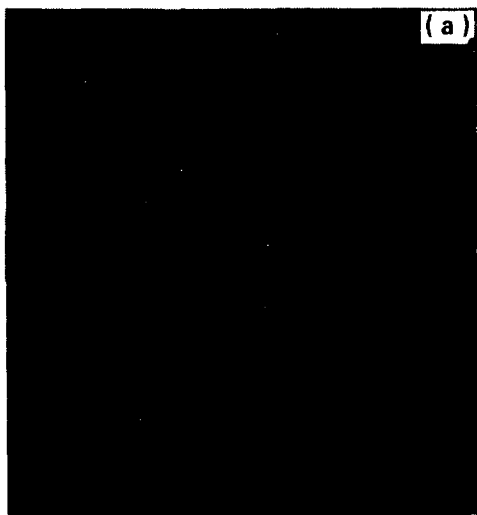


Fig. 9 Surface morphology of implanted (300 keV , $3 \times 10^{12} \text{ Se}^+/\text{cm}^2$) semi-insulating GaAs samples after (a) implantation and after irradiation with an electron beam pulse of energy density, (b) 0.42 J/cm^2 , (c) 0.67 J/cm^2 , and (d) 1.05 J/cm^2 .

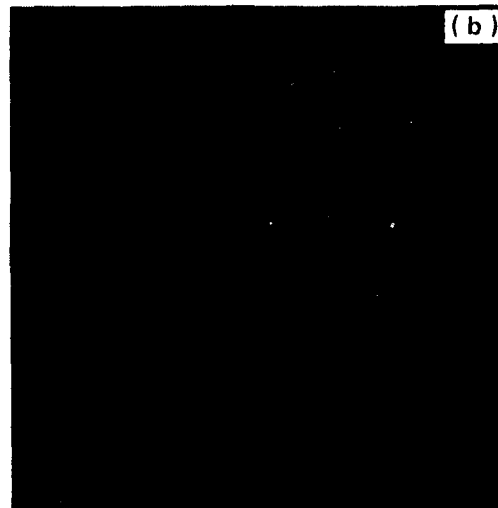


Kr \rightarrow GaAs, R. T., 300 keV, $1 \times 10^{15} \text{ cm}^{-2}$ ELECTRON
BEAM ANNEAL, NO ENCAPSULANT

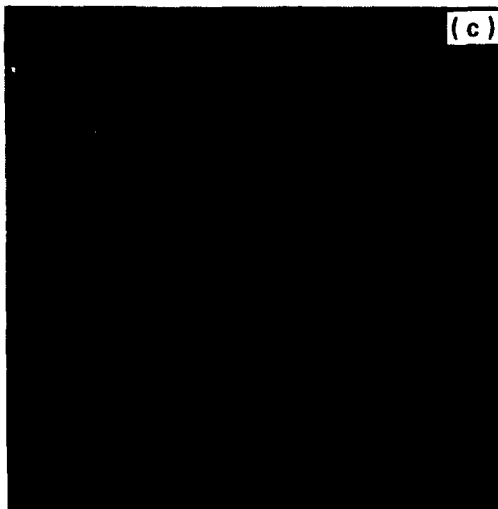
SC79-4284



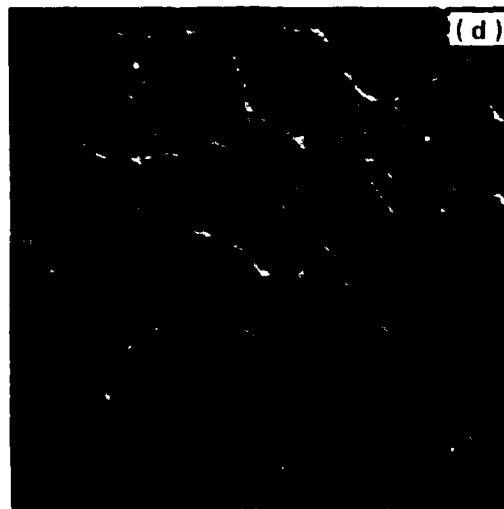
NO ANNEAL



0.42 J/cm²



0.67 J/cm²



1.05 J/cm²

20 μm

Fig. 10 Surface morphology of implanted (300 keV , $1 \times 10^{15} \text{ Kr}^+/\text{cm}^2$) semi-insulating GaAs samples after, (a) implantation and after irradiation with an electron beam pulse of energy density, (b) 0.42 J/cm^2 , (c) 0.67 J/cm^2 , and (d) 1.05 J/cm^2 .



ions (see Fig. 9). The sample irradiated with an electron beam pulse of 0.67 J/cm^2 (Fig. 10c) shows a surface which is indistinguishable from the surface of the as-implanted samples (Fig. 10a), except for the color change due to the recrystallization of the amorphous layer. Pits such as seen on the surfaces of low dose implanted samples after electron beam irradiation (Figs. 9c and d) were almost absent on the surfaces of high dose implanted samples irradiated with similar energy densities of electron beam pulses (Figs. 10c and d). The type of surface structure (Fig. 10d) indicates that some kind of damage is introduced by the electron beam pulse of 1.05 J/cm^2 in the high dose implanted samples. This kind of structure was not found on the surfaces of low dose implanted and electron beam irradiated samples (see Fig. 9). From this surface morphology study of electron beam irradiated samples, it was quite clear that in order to achieve effective annealing of ion implanted semi-insulating GaAs without introducing additional damage, the energy density of the electron beam pulse should be adjusted according to the ion implantation dose.

3.2 Structural and Compositional Studies

Semi-insulating, Cr-doped GaAs wafers of $\langle 100 \rangle$ orientation were implanted at room temperature with 300 keV Kr^+ ions to a (high) dose of 10^{15} cm^{-2} , or with 300 keV Se^+ ions to a (low) dose of $3 \times 10^{12} \text{ cm}^{-2}$. The $\langle 100 \rangle$ axis of the wafers was offset by $\sim 7^\circ$ with respect to the beam during implantation. The unencapsulated wafers were cleaved into several samples which were each irradiated with a single electron beam pulse in vacuum. Channeling measurements were taken by using a 2.4 MeV He^+ beam incident on samples over areas typically 1 mm x 2 mm. TEM studies were performed on the same samples in "plan" view.

Results of channeling and TEM analysis are given in Figs. 11 and 12. The unirradiated, high dose Kr^+ implanted sample had a 2200Å thick amorphous surface layer (Fig. 11a). The As/Ga ratio at the surface, obtained from the random backscattering spectrum, was close to unity. TEM plan view

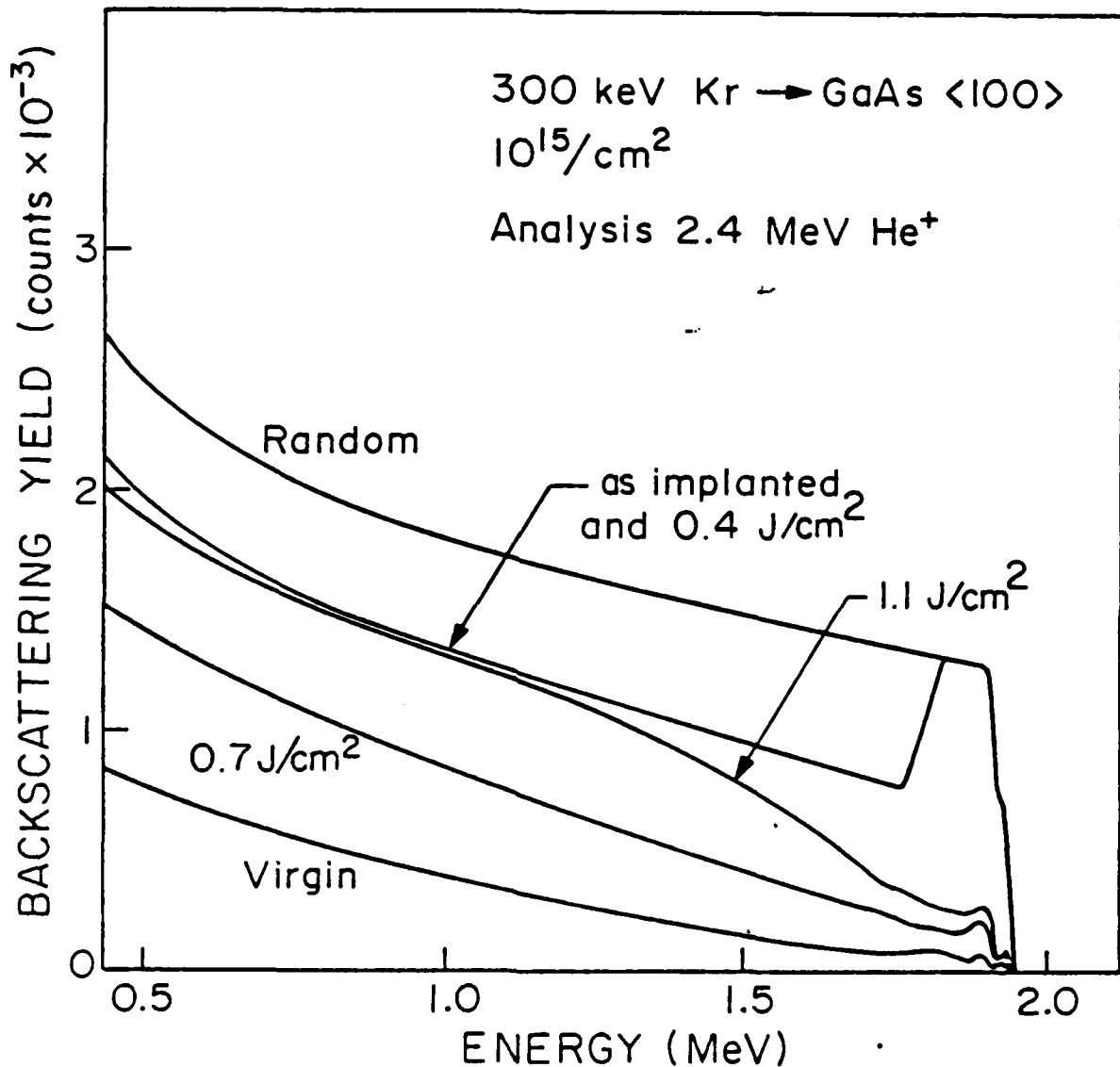
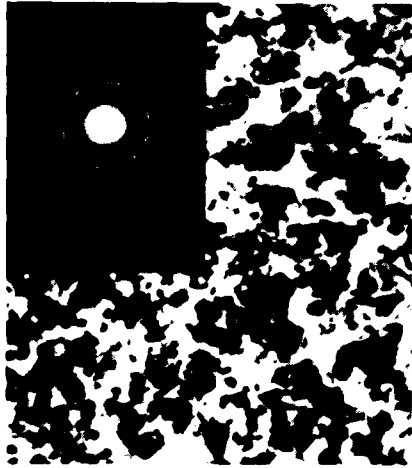


Fig. 11a Energy spectra of 2.4 $^4\text{He}^+$ ions backscattered from $\langle 100 \rangle$ GaAs, implanted at room temperature with 300 keV, 10^{15} Kr $^+$ /cm 2 , before and after single-pulse electron beam irradiations at the indicated fluences. The random spectrum is for the as-implanted (unirradiated) sample. The aligned spectrum from a virgin sample (unimplanted and unirradiated) is shown for comparison. The Kr signal is too small to be observed in all cases.



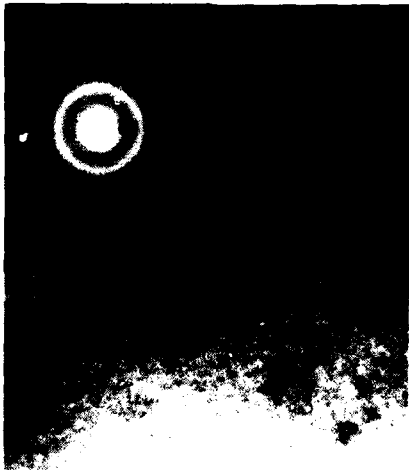
SC79-5244



0.4 J/cm²



1.1 J/cm²



AS IMPLANTED



0.7 J/cm²

0.4 μm

Fig. 11b TEM micrographs for the same samples as in Fig. 11a.

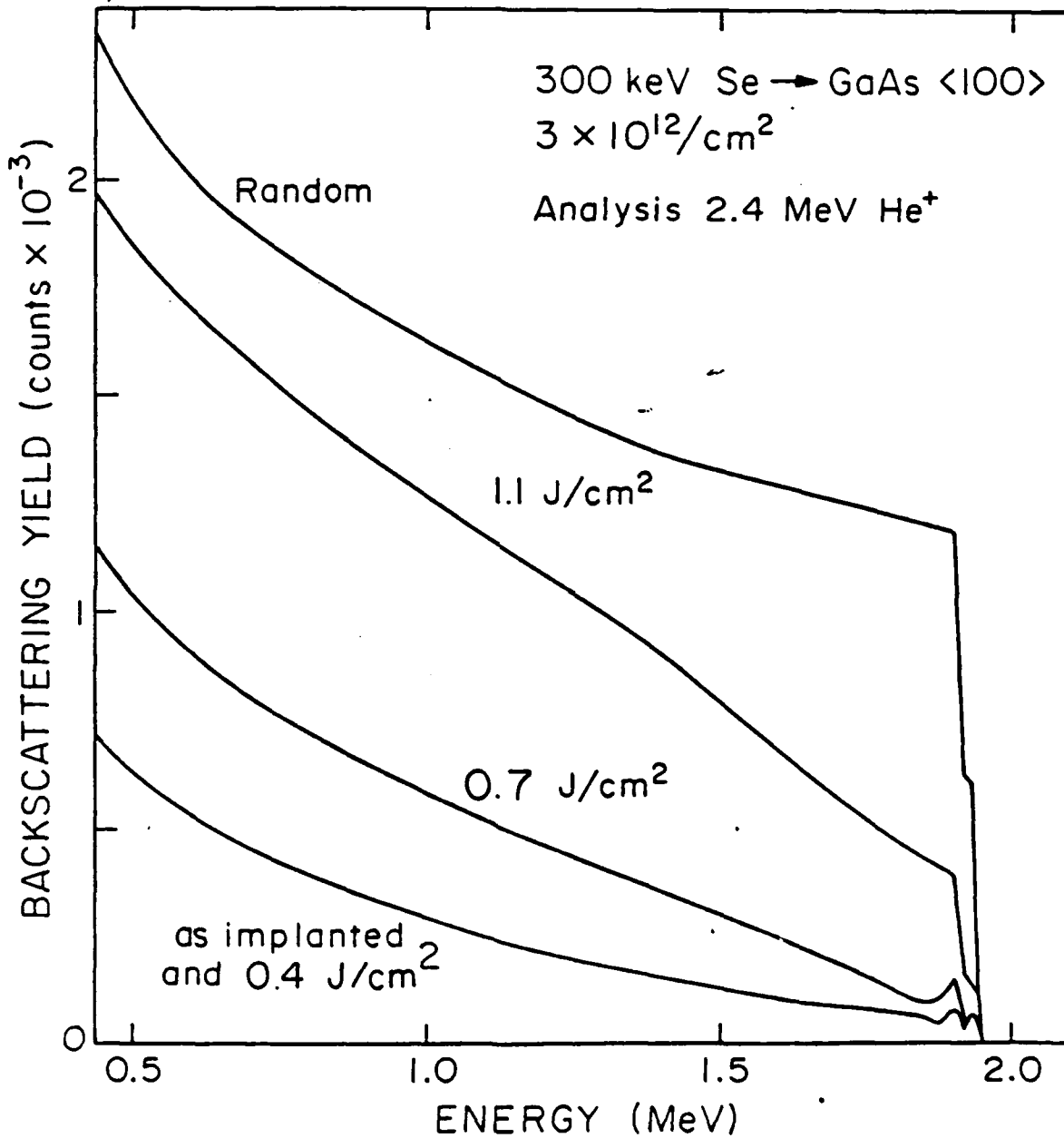
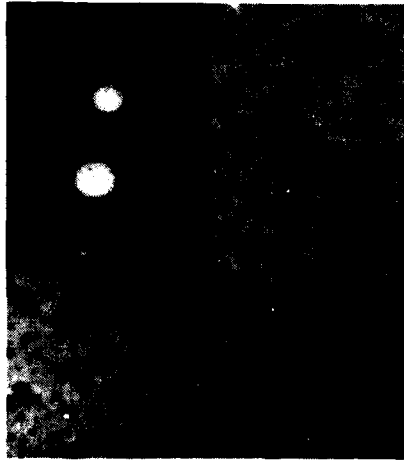


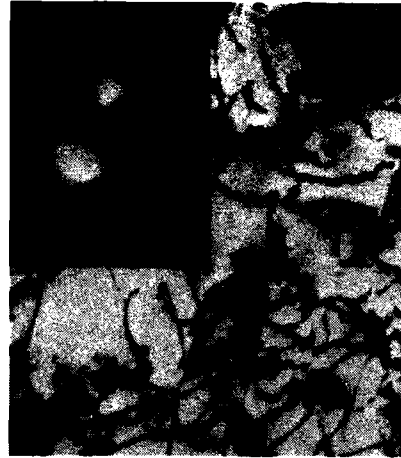
Fig. 12a Energy spectra of 2.4 MeV $^4\text{He}^+$ ions backscattered from $\langle 100 \rangle$ GaAs, implanted at room temperature with 300 keV, $3 \times 10^{12} \text{ Se}^+/\text{cm}^2$, before and after single-probe electron beam irradiations at the indicated fluences. The random spectrum is for the as-implanted (unirradiated) sample. The spectrum for a virgin sample (unimplanted and unirradiated) cannot be distinguished from the one for the as-implanted sample on this scale. The Se signal is too small to be observed in all cases.



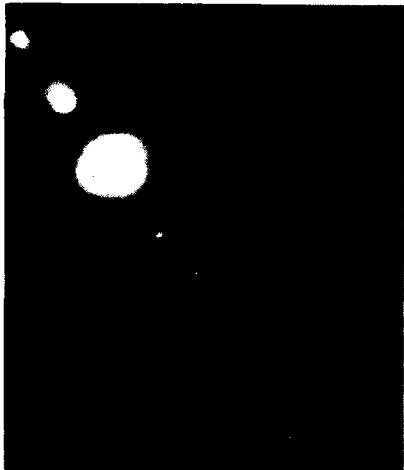
SC79-5245



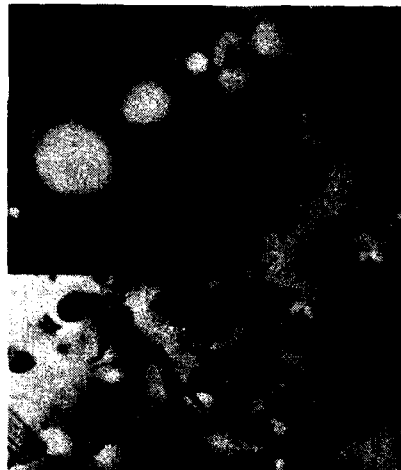
0.4 J/cm²



1.1 J/cm²



AS IMPLANTED



0.7 J/cm²

0.4 μm

Fig. 12b TEM micrographs for the same samples as in Fig. 12a.



showed the damage as a featureless structure (Fig. 11b), and the transmission electron diffraction (TED) pattern confirmed the existence of the amorphous layer (Fig. 11b). After a pulsed electron irradiation of 0.4 J/cm^2 , the aligned spectrum was the same as before irradiation (Fig. 11a). However, TEM results showed that the irradiated layer had a grainy structure with mean grain size $\sim 1000 \text{ \AA}$ (Fig. 11b). The TED pattern indicated the existence of a polycrystalline layer (Fig. 11b). After a 0.7 J/cm^2 irradiation, the channeling yield at the surface, x_0 , had dropped from 1.00 to 0.11 (Fig. 11a), indicating rather good crystalline quality. Comparison with the aligned spectrum for a virgin crystal (i.e., unimplanted and unirradiated), for which $x_0 = 0.04$ in the setup used in this work, showed that some disorder was present after a 0.7 J/cm^2 pulse. The surface of the irradiated sample was found to be Ga rich (As/Ga=0.8). TEM (Fig. 11b) indicated the existence of dislocation lines and gray patches in the regrown layer. TED indicated that the layer was now a single crystal (Fig. 11b). At a still higher electron fluence of 1.1 J/cm^2 , the surface channeling yield was 0.17, and a high dechanneling rate indicated the presence of extended defects down to a depth greater than $1 \mu\text{m}$ (Fig. 11a). The As/Ga ratio at the surface was ≈ 0.8 . TEM showed a high density of dislocations and the presence of microcracks (Fig. 11b). TED indicated the material was still a single crystal. To summarize the observations of electron beam pulsed annealing of high dose (10^{15} cm^{-2}) Kr^+ implanted GaAs, it was noted that at low energy density (0.4 J/cm^2), the recrystallization of the amorphous layer gave rise to the formation of polycrystalline material. Electron irradiation pulsing of 0.7 J/cm^2 or higher resulted in single crystalline layers with increasingly higher density of dislocations. The optimum energy density for successful recrystallization seems to lie between 0.4 and 0.7 J/cm^2 for the pulsed electron beam parameters chosen.

Figure 12 shows the results of measurements performed on the low dose ($3 \times 10^{12} \text{ cm}^{-2}$) Se^+ implanted and pulsed electron beam irradiated samples. Both the unirradiated and the 0.4 J/cm^2 irradiated samples exhibited a x_0 value of 0.05, almost as good as a perfect single crystal (Fig. 12a). The surface composition was stoichiometric. However, TEM examination (Fig. 12b)



of the 0.4 J/cm^2 irradiated sample revealed the existence of disordered zones (gray patches) with some probable Ga precipitates (black dots).¹² After a 0.7 J/cm^2 pulse irradiation, x_0 increased to 0.07, the channeled spectrum was found to be well above that for the unirradiated sample, and the surface As/Ga ratio was 0.75. TEM analysis (Fig. 12b) revealed Ga rich regions (black patches and dots) and the irradiated layer was found to possess dislocation lines and stacking faults. TED showed that the layer was still single crystalline. At an electron fluence of 1.1 J/cm^2 , x_0 reached 0.31 (Fig. 12b), and the shape of the channeled spectrum indicated a heavily disordered structure. The As/Ga ratio at the surface was ≈ 0.7 . A TEM micrograph for this sample (Fig. 12b) exhibited a dense dislocation network, probably arising from high thermal stresses produced by rapid temperature change.

In summary, the recrystallization and annealing of implanted GaAs layers by a pulsed electron beam can be interpreted as occurring via liquid phase regrowth. The existence of a threshold for the annealing of amorphous layers was observed; for the electron beam parameters chosen, the annealing threshold ranged between 0.4 and 0.7 J/cm^2 for a 2200Å amorphous layer created by a room temperature 300 KeV $10^{15} \text{ cm}^{-2} \text{ Kr}^+$ implantation. Below the threshold, at 0.4 J/cm^2 , it appeared that the electron beam pulse induces melting of the amorphous layer, but the melt depth did not penetrate the entire 2200Å of the amorphous layer, thus leading to polycrystalline regrowth on an underlying heavily damaged layer. Above the threshold, melting of the entire amorphous layer took place, leading to epitaxial regrowth on single crystalline substrate. These observations are in agreement with analogous studies performed on laser-annealed samples (see Section 2).¹³⁻¹⁵ Crystalline (or slightly damaged) layers irradiated with an electron beam pulse of 0.4 J/cm^2 or higher possessed lattice defects. It is interesting to note that electron beam pulsing at a fluence of 0.7 J/cm^2 produced more damage in the high dose, amorphous implanted layer than in the low dose case, as seen in the respective channeling spectra. This effect can be explained as follows. The absorption of energy deposited by the electron beam is not expected to depend significantly on the microstructure of the material. However, the thermal properties



ERC41008.11FR

of the layers, namely the latent heat of fusion and the melting temperature, which control the melt depth and the duration for which the layer remains molten, may be different in the two cases. A similar dependence for electron beam irradiation of implanted layers in Si has been previously observed.¹⁶ Amorphous or heavily damaged layers would have a lower heat of fusion than crystalline material. Thus, for equal electron beam fluence, an amorphous layer would melt deeper and stay molten longer than a crystalline layer. Observations indicated a significant loss of As at the surface after a 0.7 J/cm^2 pulse irradiation. Thus, as already pointed out by Tsu et al.,¹⁷ the regrowth would take place from a Ga-rich liquid, which may account for some of the disorder. These effects were even more pronounced for 1.1 J/cm^2 irradiations. It appeared that a judicious choice of electron beam parameters (such as fluence, pulse length, and energy distribution) could be found which would optimize the annealing process in GaAs.

3.3 Electrical Measurements

Resistivity and Hall effect measurements were made on Se implanted semi-insulating GaAs samples after irradiation by electron beam pulses. For the measurements, an area of about $7 \text{ mm} \times 7 \text{ mm}$ within the irradiated region was used to etch a Van der Pauw type mesa provided with Au-Ge/Pt alloyed ohmic contacts. In some cases, differential Hall effect measurements of the striping type were also performed to determine the depth distribution of electron concentrations.

In Fig. 13, sheet electron concentration (N_S), effective mobility (μ_e), and sheet resistance (ρ_S) measured in several samples are plotted against the incident energy density of pulsed irradiation from the electron beam. All samples were implanted with $10^{15} \text{ 300 keV Se}^+$ ions/cm² at room temperature prior to annealing. All anneals were performed without an encapsulant. The values of N_S , μ_e , and ρ_S measured in samples capped with AlN and thermally annealed are also shown in Fig. 13 as dotted lines for comparison. The thermally annealed sample was implanted with a similar dose and energy of



ERC41008.11FR

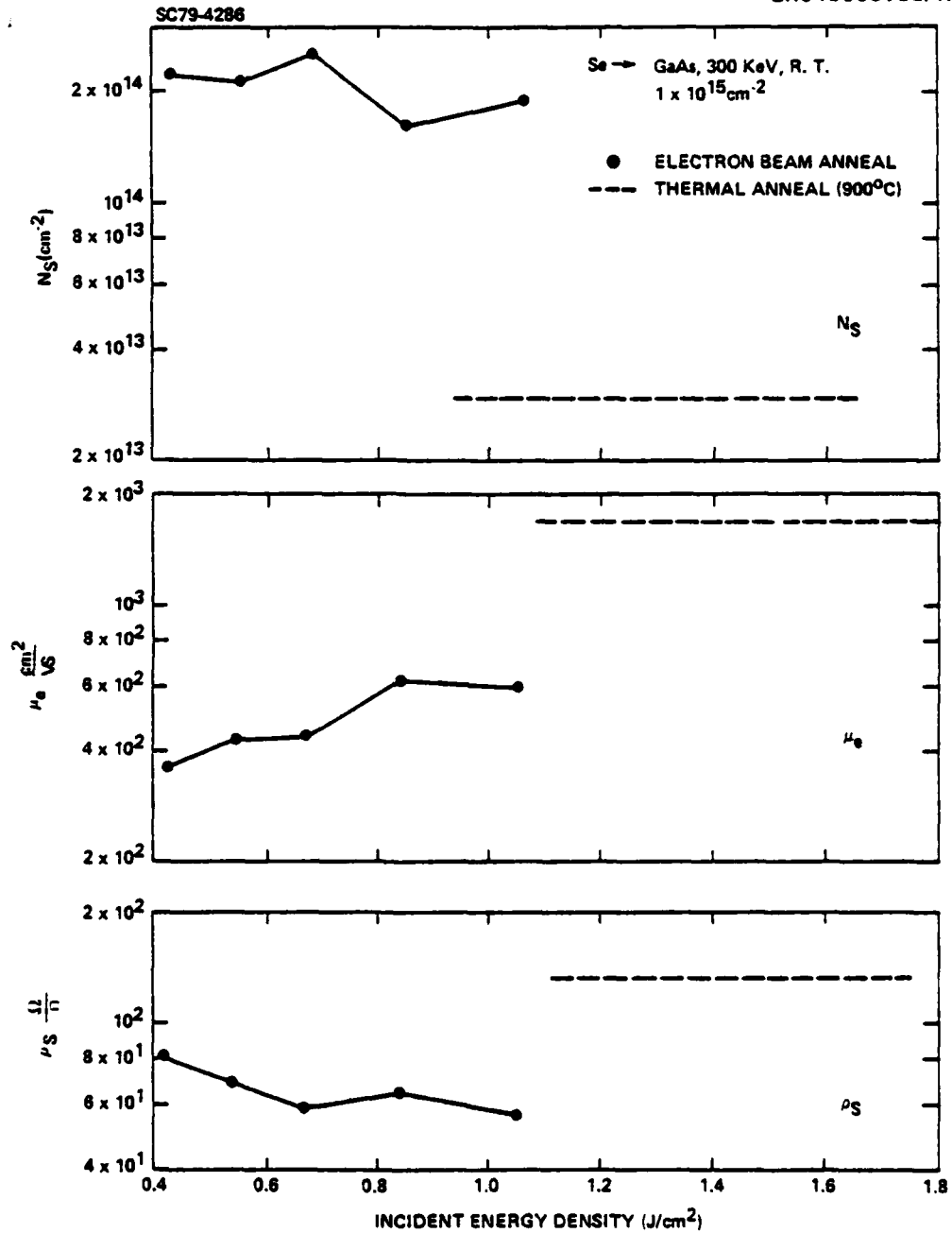


Fig. 13 Sheet electron concentration (N_S), effective mobility (μ_e) and sheet resistance (ρ_S) measured in the pulse-annealed GaAs samples vs the incident energy density of electron beam irradiation. All samples were implanted with 300 keV, $1 \times 10^{15} \text{Se}^+/\text{cm}^2$ at room temperature prior to pulse-annealing. As a comparison, values of N_S , μ_e and ρ_S measured for a thermally annealed sample are also shown by dotted lines. The thermally annealed sample was implanted with a similar dose and energy of Se ions and capped with a film of AlN prior to annealing in H_2 ambient at 900°C for 10 min.



Se ions at 350°C, and the annealing was performed at 900°C for 10 min. in H₂ ambient. All the electron beam annealed samples showed higher activation of Se ions (higher values of N_S) when compared to the thermally annealed sample. Figure 14 gives depth profiles of electron concentration (N) and mobility (μ) for two samples implanted with 10¹⁵ 300 keV Se⁺ ions/cm² and annealed with two different energy densities of the electron beam pulse, one with 0.42 J/cm² and the other with 0.67 J/cm² (see Fig. 13). The electron concentration profiles exhibited similarities in the two cases, and they appeared deeper than the LSS calculated profile.⁹ The peak electron concentrations were found to reach levels higher than 10¹⁹/cm³, as were also measured in the laser annealed samples (see Section 2).

Several samples implanted with lower doses ($3 \times 10^{12} - 1 \times 10^{14}/\text{cm}^2$) of 300 keV Se⁺ ions were also irradiated with the electron beam pulses of similar energy densities as employed for annealing the 10¹⁵/cm² implants. These samples showed poor or no activation of the implanted Se. As an example, a 10¹⁴/cm² implant exhibited an activation of only 6.1% after irradiation with an electron beam pulse of 0.67 J/cm².¹⁸

In order to understand the role of damage introduced by the electron beam in affecting the electrical properties of the irradiated layers, electron beam irradiations of activated layers in semi-insulating GaAs were performed. Cr-doped GaAs samples, implanted with 400 keV Se ions to a dose of 10¹³ cm⁻², were first thermally annealed in H₂ at 850°C for 30 min, using a Si₃N₄ cap, to activate the implanted Se, and then electron beam irradiated with the cap removed. The sheet-resistance, which was 410 Ω/□ prior to irradiation, increased to 500 Ω/□ for a 0.63 J/cm² pulse. These measurements indicate that with the electron beam parameters chosen, crystalline defects are introduced by irradiation, degrading the electrical activity in the conducting layers.

Further experiments were carried out to determine whether the initial crystalline structure of the low dose implanted layer was responsible for the lack of electrical activity. For this study, 300 keV, 3 × 10¹² Se/cm² ions were implanted into a layer previously amorphized by a 300 keV, 10¹⁵ Kr⁺/cm²

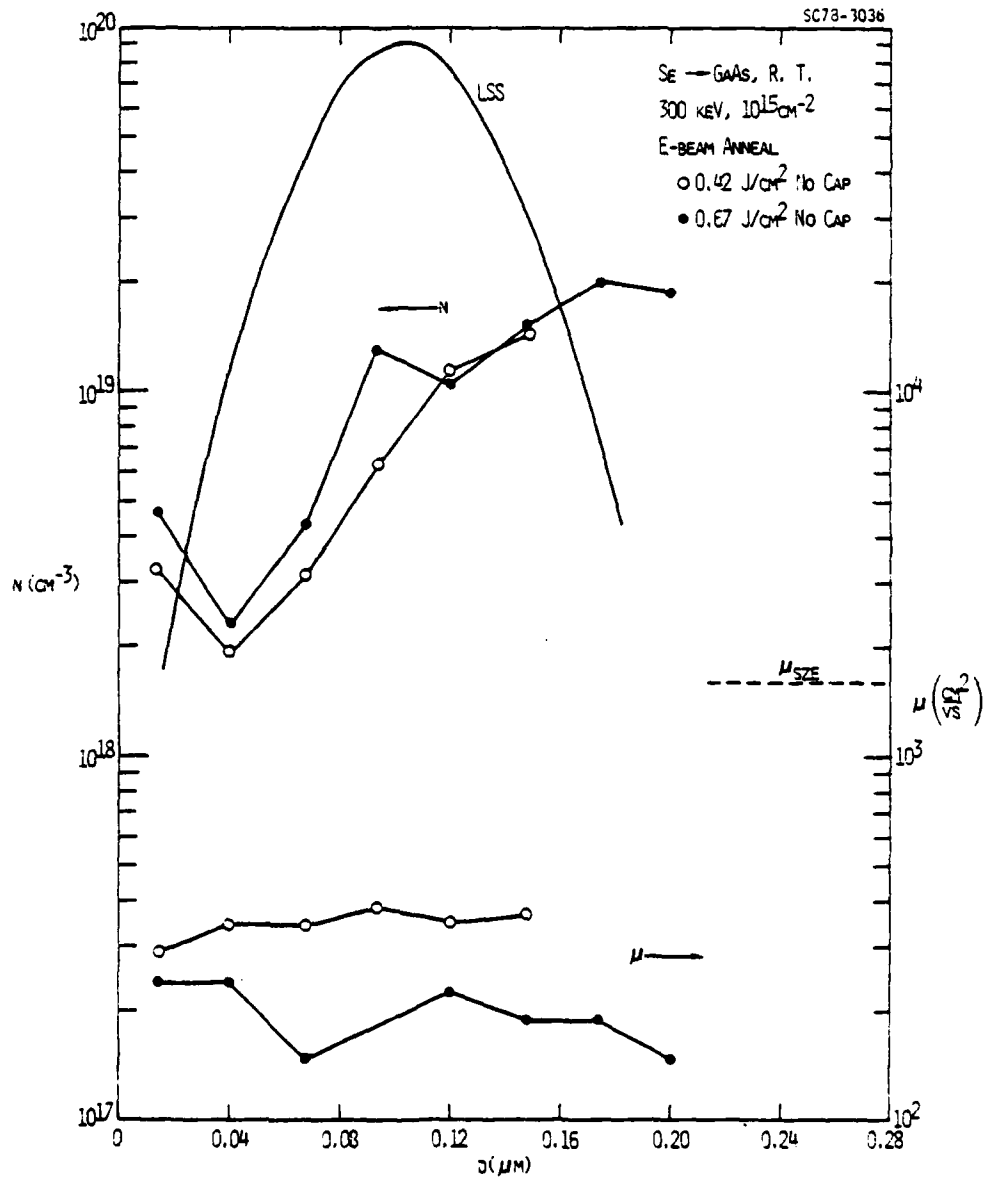


Fig. 14 Electron concentration (n) and mobility (μ) vs depth (d) profiles of two electron beam annealed samples, one with a pulse of 0.42 J/cm^2 (○) and the other with a pulse of 0.67 J/cm^2 (●). Both samples were implanted with 300 keV, $1 \times 10^{15} \text{ Se}^+$ ions/cm at room temperature prior to electron beam exposure. The dotted line (μ_{SZE}) represents the estimated value of mobility¹⁰ for the peak electron concentration measured in the n -profile.



ERC41008.11FR

implant. Again, no electrical activity could be detected after pulsed electron beam irradiation in these samples.

In an attempt to investigate the possible influence of the Cr distribution on the measured electrical activity in the implanted and irradiated layers, atomic depth profiles of Cr and Se were measured by SIMS. The results are given in Figs. 15 and 16. For both high (10^{15} Se/cm² - Fig. 15) and low (10^{13} Se/cm² - Fig. 16) dose, 300 keV implants into Cr-doped GaAs, there was far less redistribution of Cr after a pulsed electron irradiation of 0.54 J/cm² than that observed after capped thermal annealing.¹⁹⁻²¹ Also, the Se profiles did not change significantly after pulsed electron irradiation. (The enhanced signals near the surface, which were probably due to measurement artifacts arising from surface impurities, did not represent the true Se or Cr signals and therefore should be ignored for the present analysis). The electron beam fluence of 0.54 J/cm² was sufficient to electrically activate 10^{15} /cm² implanted Se ions. It should be pointed out that the distribution of Cr, which is a deep acceptor in GaAs, can significantly affect the activation of the implanted Se by compensation as has been observed for thermally annealed samples.^{19,21} The higher electrical activity measured in the high dose, 10^{15} cm⁻² Se implanted and electron beam irradiated samples, when compared with thermally annealed samples, may be partly due to insignificant accumulation of Cr in the implanted region.²⁰ Also, the poor or lack of electrical activity measured in the low dose, 10^{13} cm⁻² Se implanted and irradiated samples may be partly due to insignificant depletion of Cr near the surface.^{19,21} These statements are speculative, and more experiments are needed to clarify the possible effects of Cr distribution in affecting the electrical activity measured in Se implanted and irradiated samples.

To assess further the possible role of Cr, the low dose Se implants were repeated in nominally undoped, vapor phase epitaxial layers grown on Cr-doped GaAs. There was no detectable electrical activity after pulsed irradiation in these layers, however, since the Cr levels in the layers before and after irradiation have not been measured, no definite conclusions can be drawn.

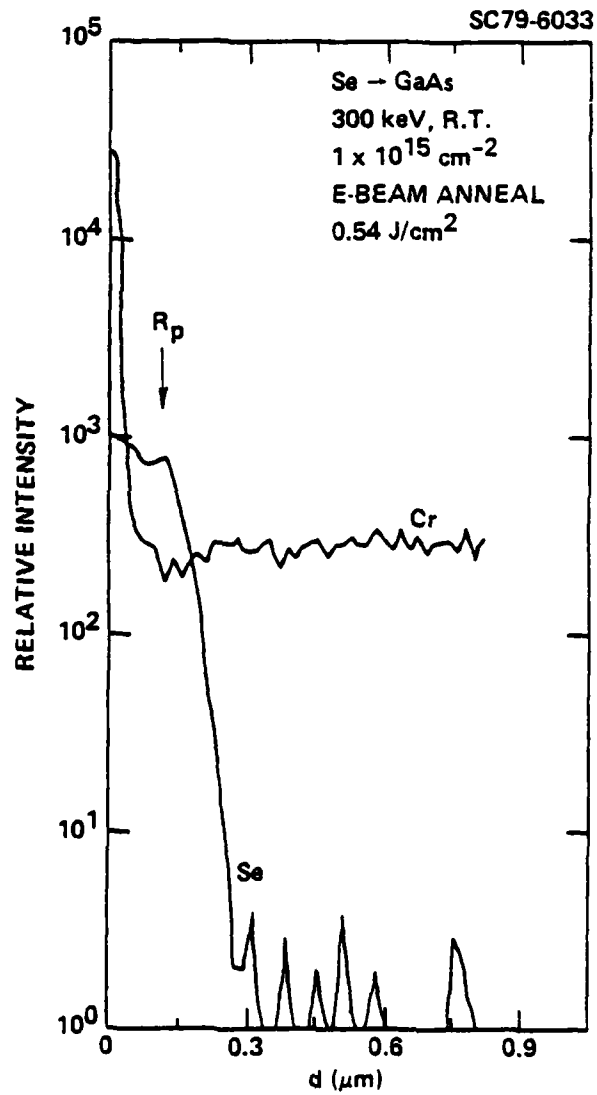


Fig. 15 Depth distributions of Se and Cr atomic concentrations measured by SIMS in a semi-insulating GaAs sample irradiated with an electron beam pulse of 0.54 J/cm^2 . The sample was implanted at room temperature with 300 keV Se^+ ions to a dose of 10^{15} cm^{-2} prior to electron beam irradiation.

ERC41008.11FR

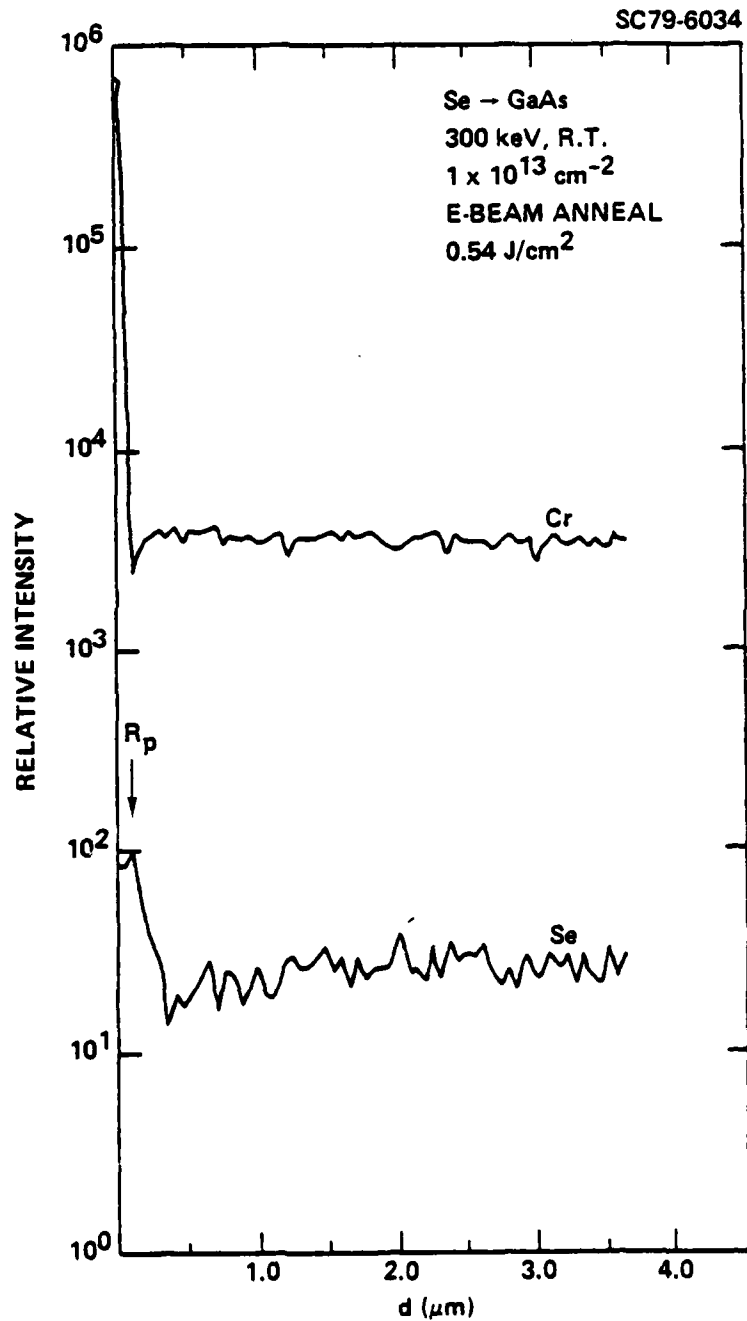


Fig. 16 Depth distributions of Se and Cr atomic concentrations measured by SIMS in a semi-insulating GaAs sample irradiated with an electron beam pulse of 0.54 J/cm^2 . The sample was implanted at room temperature with 300 keV Se^+ ions to a dose of 10^{13} cm^{-2} prior to electron beam irradiation.



ERC41008.11FR

In summary, the recrystallization mechanism of amorphous layers in GaAs by means of short (100 ns) electron beam pulses appeared to be well understood. On the other hand, low dose ($<10^{13}$ cm⁻²) Se implants into either single crystal or amorphous, Cr-doped or nominally undoped GaAs, could not be electrically activated by means of short pulses at present. The exact reasons are not clear.



4.0 PULSED ELECTRON BEAM ALLOYING OF Au-Ge/Pt OHMIC CONTACTS TO n-TYPE GaAs

The performance of various GaAs devices can depend substantially on the quality of ohmic contacts which provide the means for coupling external signals to the devices concerned. Ohmic contacts with low r_c aid in improving the frequency characteristics, noise properties, and power capability of active components fabricated on GaAs. In addition to possessing low r_c , it is desirable that the contacts be uniform, reliable and reproducible. Although considerable effort has been spent over the last decade in achieving uniform, reliable, low r_c contacts to n-type GaAs,²² the best values of r_c ($\sim 10^{-6} \Omega\text{-cm}^2$)²³ have been significantly higher than what one normally obtains with e.g., silicide contacts on Si ($r_c \sim 10^{-7} \text{ cm}^2$).²⁴ Various metal systems have been explored with different thermal cycles.²² In the majority of the cases, two basic approaches have been used which have yielded ohmic contacts upon appropriate heat treatments: one utilizes an Au-base eutectic system (e.g., Au-Ge, Au-Sn, Au-Si, Au-In, Au-Te) with Ni or Pt added to avoid the loss of surface wetting. During melting and subsequent resolidification,²² the other uses noneutectic mixtures (e.g., Ge/Pd).²⁵ Ohmic contact formation in the former case has been attributed to the melting of the eutectic alloy, dissolution of GaAs in the metals and regrowth of heavily doped GaAs upon subsequent cooling. For the latter case, the contact formation is believed to involve a solid-phase reaction between the metals and GaAs. In either case, the main problem in obtaining low r_c contacts has been the difficulty in generating a heavily doped n-type GaAs layer at the metal-GaAs interface.

Recently, several techniques have been used to produce heavily doped shallow n-type GaAs layers for low r_c ohmic contacts. These have included growing doped layers with molecular beam epitaxy,²⁶ generating layers by dual implantation (e.g., Se and Ga) followed by thermal annealing,²⁷ and producing layers by high dose ($>10^{15} \text{ cm}^{-2}$) donor implantation, followed by subsequent annealing by pulsed laser²⁸ or electron beams.²⁹ In addition, laser beams have also been used to directly alloy ohmic contacts to GaAs,³⁰⁻³² although the r_c values have not been very encouraging. To the authors' knowledge the



ERC41008.11FR

best reported contacts ($r_c < 6 \times 10^{-7} \Omega\text{-cm}^2$)* have been the non-alloyed type on a very heavily doped ($n_{\text{peak}} = 2 \times 10^{10} \text{ cm}^{-3}$) GaAs layer generated by a 120 keV $5 \times 10^{15} \text{ cm}^{-2}$ Se implant followed by pulsed electron beam annealing.²⁹

In this section direct alloying of Au-Ge/Pt contacts to n-type GaAs by a single pulse from an electron beam is reported. The ohmic character of the contacts was presumably realized by the heavy n-type doping of a thin GaAs layer by Ge at the metal-GaAs interface during the alloying process. From the point of view of energy absorption necessary to alloy contacts, pulsed electron beams should be preferable to pulsed laser beams because high optical reflectivity of the metals is not of major concern for electrons.

Wafers of semi-insulating $\langle 100 \rangle$ GaAs were implanted at room temperature with 400 keV Se^+ ions to a dose of $1 \times 10^{13} \text{ cm}^{-2}$. During implantation the ion-beam was oriented $\sim 7^\circ$ off the sample's normal to minimize channeling effects. After implantation, the samples were coated with $\sim 2000\text{\AA}$ of reactively sputtered Si_3N_4 film and subsequently annealed in H_2 at 850°C for 30 min. to generate an electrically active layer. Using LSS parameters with a Gaussian approximation,⁹ assuming no diffusion and 100% activation of the implanted Se, the electron concentration profile in these samples was expected to reach a peak value of $\sim 7 \times 10^{17} \text{ cm}^{-3}$ located at $\sim 0.14 \mu\text{m}$ below the surface with a standard deviation of $\sim 0.06 \mu\text{m}$. The Si_3N_4 films were removed in HF and patterns were defined photolithographically conforming to the transmission line mode (TLM) method³³ for contact resistance measurements. Preparation of such samples involved two mask steps. In the first step rectangular strips of the electrically activated layers were modified and isolated from each other by mesa-etching (see Fig. 17). In the second step, square windows were opened in the photoresist on the rectangular active layer regions. Finally, a pattern consisting of square metal pads separated by varying distances was

*The value of $r_c = 2.9 \times 10^{-7} \Omega\text{-cm}^2$ in Ref. 6 is questionable because of the relation used for computation. The time value of r_c calculated by using the relations in Ref. 13 should be $\sim 1 \times 10^{-6} \Omega\text{-cm}^2$.



ERC41008.11FR

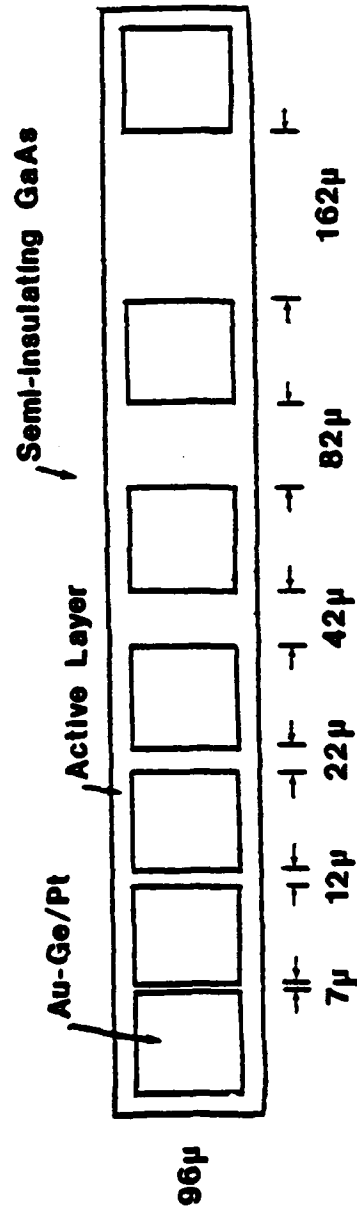


Fig. 17 Contact pattern used for specific contact resistance (r_c) measurements. This pattern was repeated numerous times on each wafer.



ERC41008.11FR

generated on the active layer regions by evaporation and lift-off of the photoresist. Prior to metal depositions, the exposed GaAs surface in the photoresist windows was briefly treated with HCl and a few hundred angstroms of the active layer were removed by employing a sequence of brief duration dips in $\text{H}_2\text{O}_2 + \text{NH}_4\text{OH}$ and $\text{H}_2\text{O} + \text{NH}_4\text{OH}$ solutions. The metals were deposited by electron beam evaporation at an approximate rate of $\sim 2.5 \text{ \AA/s}$. The metal thicknesses were 12% Ge - 88% Au = 1300Å and Pt = 300Å.

Some of the samples, as prepared above, were irradiated with single pulses from an electron beam possessing energy densities in the range of 0.2-0.9 J/cm^2 . The electron beam had a mean electron energy = 20 keV and a pulse duration, $t_p = 10^{-7}$ s. Several samples were alloyed thermally in flowing H_2 at 440°C for 2 min.

Resistance measurements between the metal pads were made by employing four tungsten probes. One set of probes was used for current biasing and the other set for voltage measurement. This method eliminated the contribution of the probe resistance in the resistance measurements. For AES measurements, a 5 keV electron beam scanned over $\sim 20 \text{ \mu m} \times 20 \text{ \mu m}$ area of the metal pads was used. Thus any nonuniformities present on the pads were averaged over the $20 \text{ \mu m} \times 20 \text{ \mu m}$ area and could not be resolved from the detected Auger signals.

Within the range of energy densities of the electron beam pulses explored, the ohmic contacts were observed after irradiation with single pulses in the range 0.3-0.7 J/cm^2 . Below 0.3 J/cm^2 there was no significant change in the I-V characteristics of the contacts after irradiation than before irradiation. Pulses $> 0.7 \text{ J/cm}^2$ resulted in non-ohmic contacts due to considerable damage to the metals and the underlying active GaAs layer. A significant increase in the sheet resistance of the underlying active GaAs layer was detected after irradiation with pulses in the 0.5-0.7 J/cm^2 range. Pulsing in the range of 0.3-0.5 J/cm^2 produced good ohmic contacts with low r_c values without significantly affecting the electrical properties of the underlying active GaAs layer.



ERC41008.11FR

Contacts alloyed with electron beam pulses with energy densities in the range $0.3-0.5 \text{ J/cm}^2$ were found to be extremely uniform with good edge definition. In Fig. 18 contact resistance measurements made on a sample irradiated with an electron beam pulse of 0.4 J/cm^2 are shown. The resistance (R) between metal pads (see Fig. 17) was plotted against the gap length (l). Each data point shown in Fig. 18 was an average of eight measurements. The bars represent the scatter in the measurements. The solid-line is a least-mean-square fitted line to the data points. The fit is extremely good. From the slope and intercept of the fitted line, the sheet resistance (ρ_s) of the underlying active GaAs layer and twice the contact resistance ($2R_c$) were computed to be $336 \text{ } \Omega/$ and $2.4 \text{ } \Omega$, respectively. Using the TLM method³³ this value of R_c corresponded to an r_c value of $4 \times 10^{-7} \text{ } \Omega\text{-cm}^2$. To the authors' knowledge, this value of r_c is one of the lowest values reported so far on ohmic contacts to n -type GaAs.

Similar contact resistance measurements made on a sample alloyed thermally in H_2 at 440°C for 2 min are shown in Fig. 19. The r_c value computed in this case was $1.3 \times 10^{-5} \text{ } \Omega\text{-cm}^2$, significantly higher than the value calculated for the pulsed electron beam alloyed contacts.

In order to explore the reasons behind the difference in r_c values between the pulsed electron beam and thermally alloyed contacts, depth profiles of the constituent element in the contacts were determined by successive sputtering and AES measurements. The samples used were those on which the contact resistance measurements had been made. In Fig. 20, AES depth profiles of the as-evaporated metals are shown. The transition of the measured signals from one metal to the other was quite abrupt, as one would expect for the as-evaporated case. AES depth profiles of the constituent elements obtained from the electron beam alloyed contacts are shown in Fig. 21. Not much intermixing of the metals with GaAs took place and the depth profiles were in general not too different from the as-evaporated case (see Fig. 20). There were, however, some differences. After pulsed electron beam alloying, a small amount of Ga from the underlying GaAs substrate had penetrated through the metallic layer

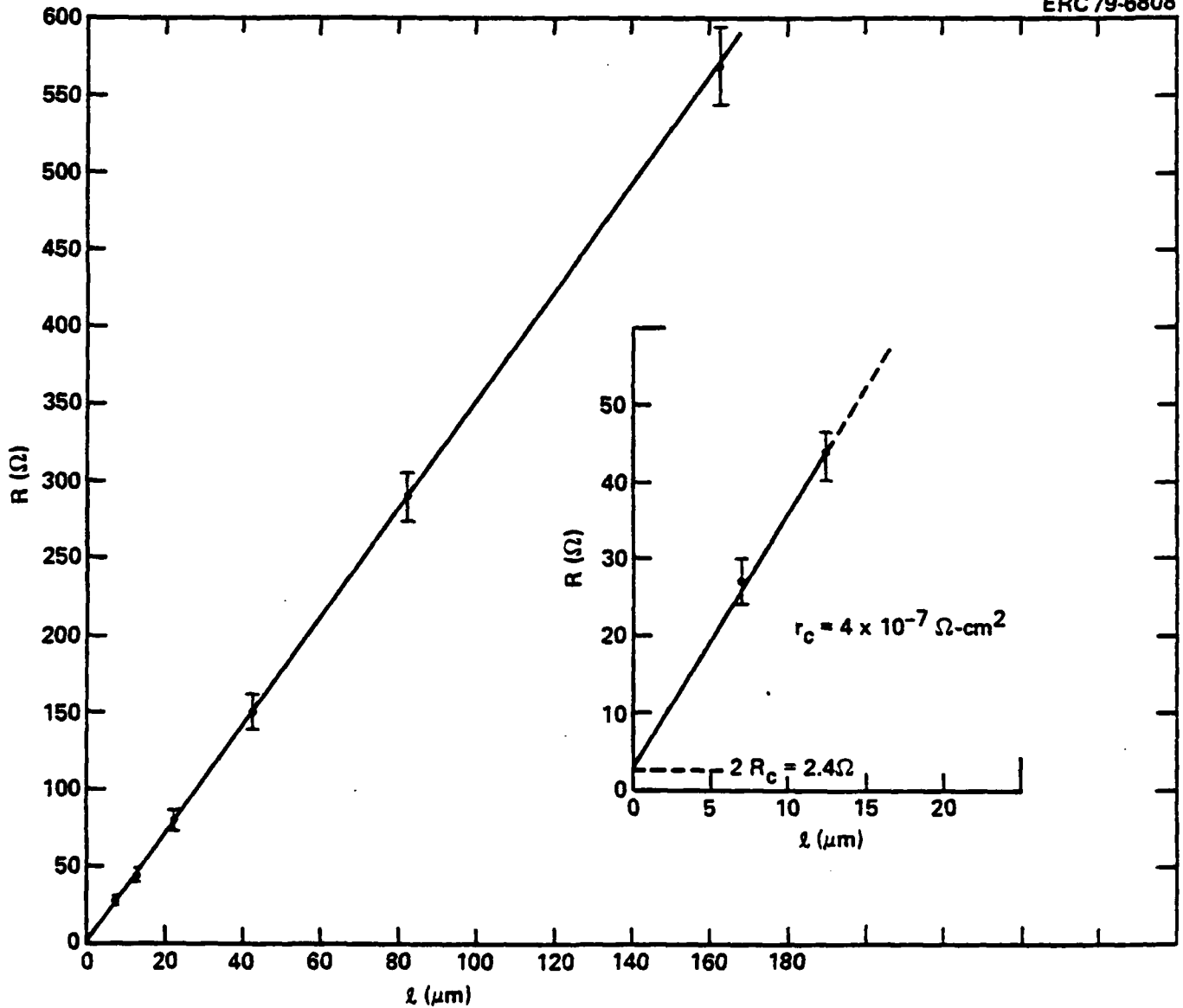


Fig. 18 Plot of resistance (R) between the metal pads as a function of gap length (l). The Au-Ge/Pt contacts were alloyed by a pulsed electron beam with an energy density of 0.4 J/cm^2 . The inset shows magnified scales near the origin.

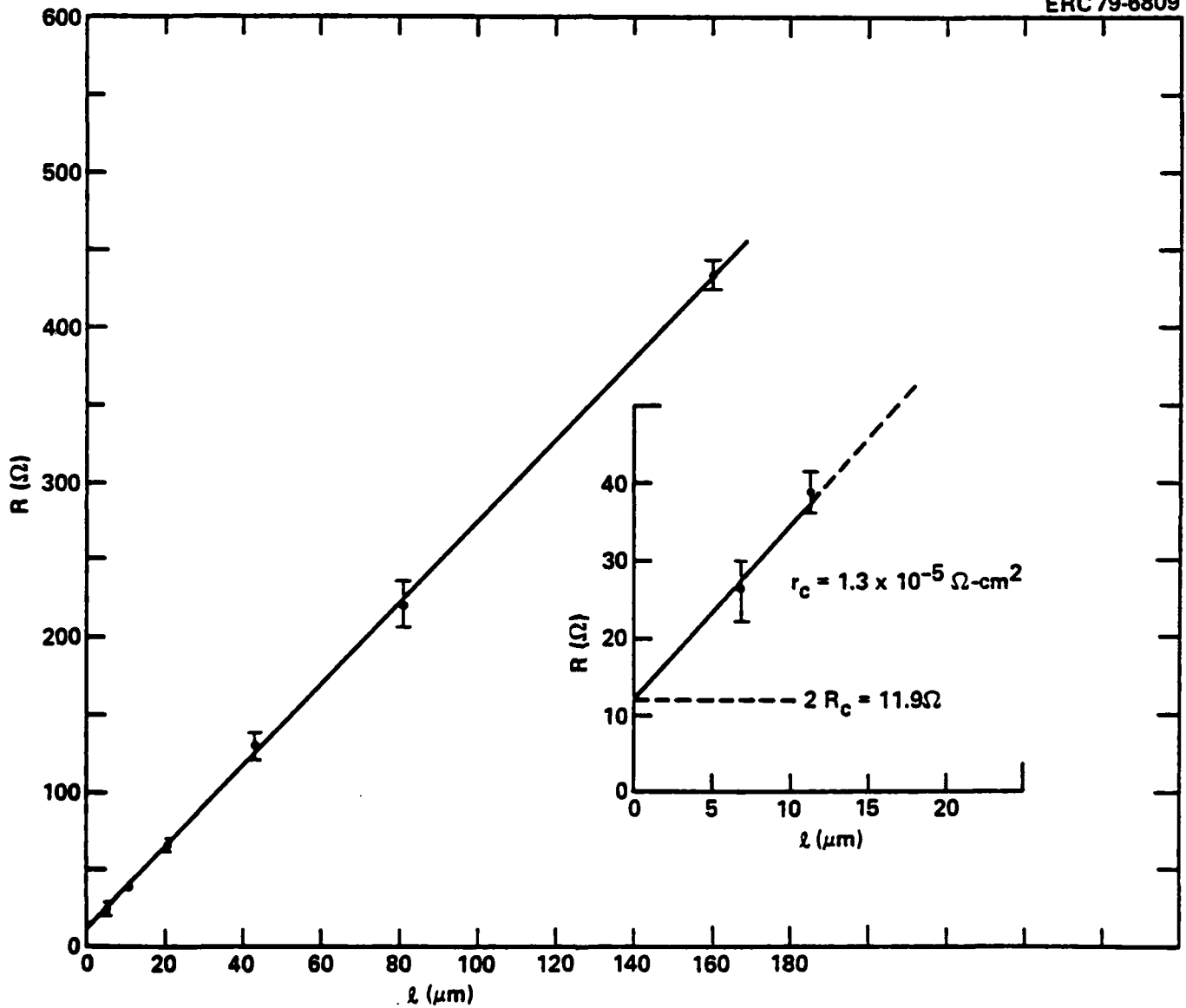


Fig. 19 Plot of resistance (R) between the metal pads as a function of gap length (l). In this case the Au-Ge/Pt contacts were alloyed thermally in H_2 at 400°C for 2 min.

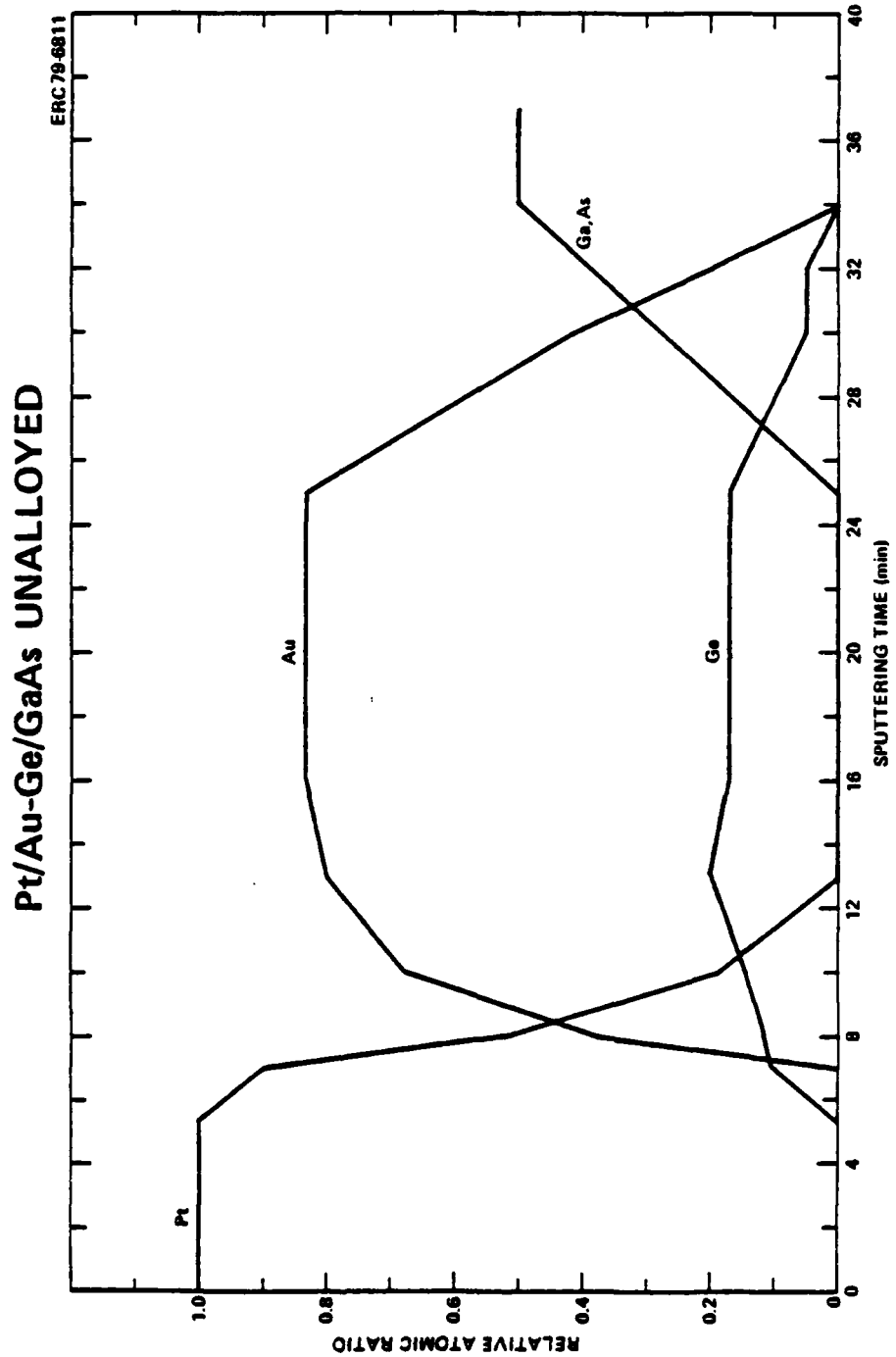


Fig. 20 AES depth profiles of the constituent elements in the unalloyed contacts.



ERC41008.11FR

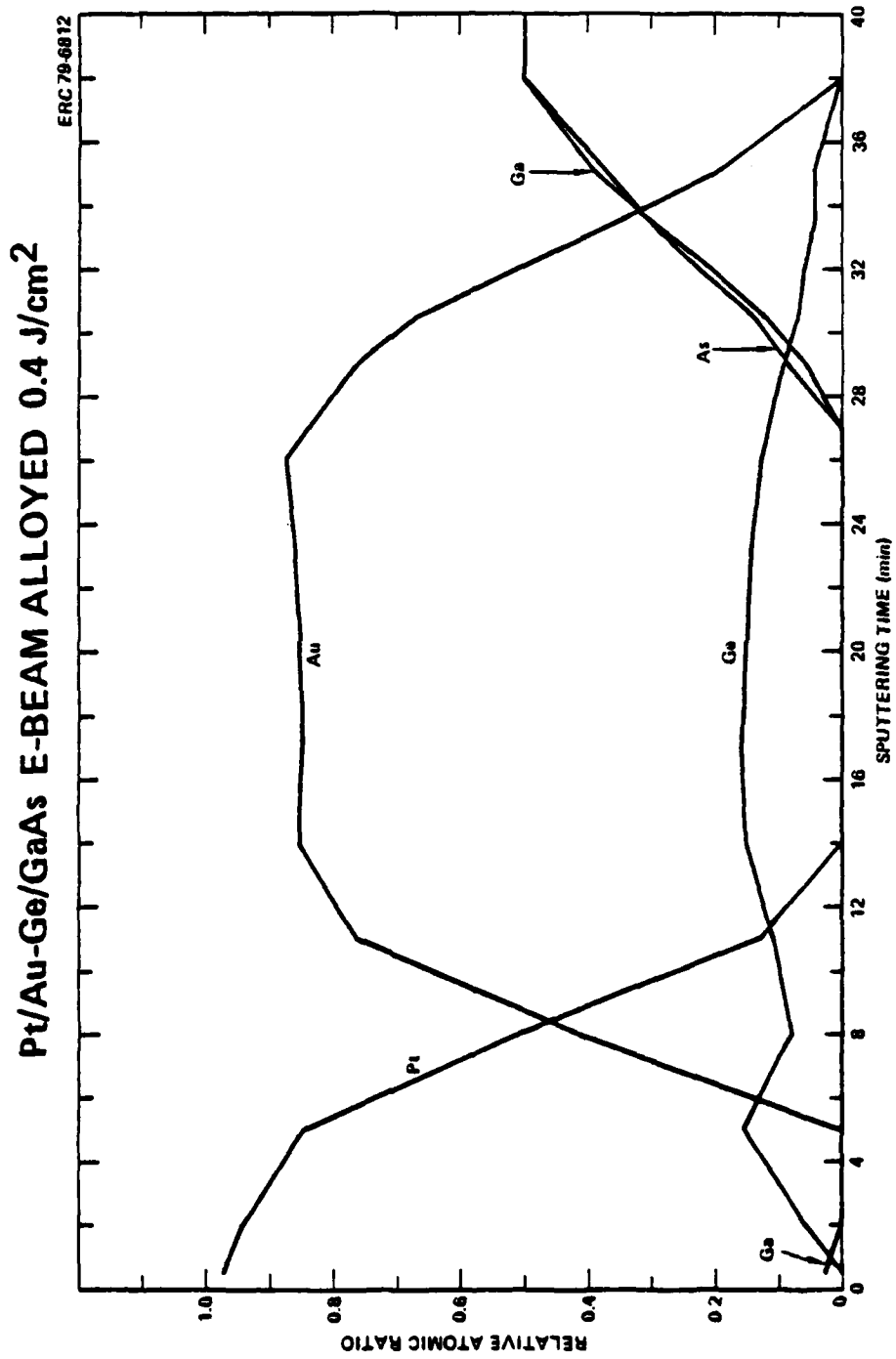


Fig. 21 AES depth profiles of the constituent elements in the contacts alloyed with electron beam pulse of 0.4 J/cm².



ERC41008.11FR

and appeared at the surface. Also, Pt and Ge had mixed, probably forming compounds. The formation of low r_c ohmic contacts in this case may be due to the generation of a very heavily doped n-type GaAs layer at the metal-GaAs interface by the replacement of Ga by Ge, without disturbing significantly the metallic layers.

In contrast to the pulsed electron beam alloyed contacts, considerable intermixing of the metals with GaAs took place for the thermally alloyed sample, as shown in Fig. 22. After thermal alloying, large amounts of Ga appeared on the surface with As distributed throughout the metallic layer. Substantial intermixing of Pt, Au and Ge was also apparent, resulting perhaps from the formation of intermetallic compounds. Higher values of r_c measured for the thermally alloyed case, compared with the pulsed electron beam alloyed case, may have resulted from the considerable amount of intermixing of the metals with GaAs during the comparatively long furnace cycle.

In summary, Au-Ge/Pt ohmic contacts alloyed to n-type GaAs by a single pulse of an appropriate energy density from an electron beam displayed a measured value for r_c as low as $4 \times 10^{-7} \Omega\text{-cm}^2$. This value was significantly lower than the $1.3 \times 10^{-5} \Omega\text{-cm}^2$ value measured on similar thermally alloyed contacts. AES measurements of the depth profiles of the constituent elements after alloying indicated that the low r_c value of the electron beam alloyed contacts may be correlated to the lack of metal intermixing with GaAs during the brief beam alloying process.

From the results reported here, it appears that Au-Ge type ohmic contacts with lower r_c values can be achieved on n-type GaAs by pulsed electron beam alloying than by thermal alloying on similarly doped samples. If the short time alloy cycle is beneficial for good contacts, a pulsed electron beam with a precisely controlled pulse duration should prove more useful than the thermal alloy cycle which can suffer from lack of the precise control of time and temperature.



ERC41008.11FR

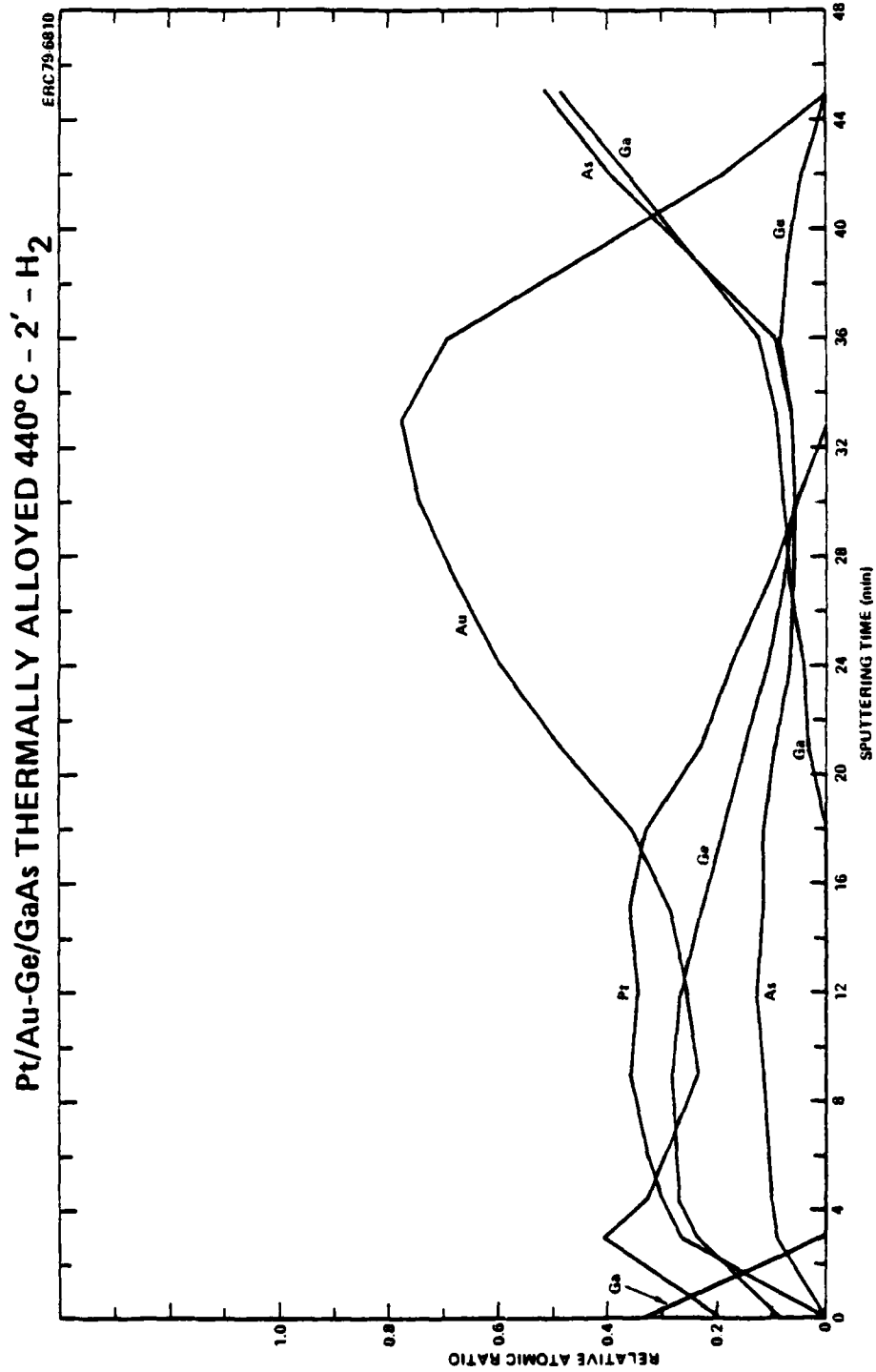


Fig. 22 AES depth profiles of the constituent elements in the contacts alloyed thermally in H₂ at 440°C for 2 min.



5.0 SUMMARY AND CONCLUSIONS

The annealing effects of a pulsed ruby laser or a pulsed electron beam on implanted GaAs have been studied. In either case, a threshold in the energy density of the pulse existed beyond which implanted amorphous layers could be successfully recrystallized. Good electrical activation of the high dose ($>10^{14}$ cm $^{-2}$) implanted donor ions in GaAs was achieved after pulsed irradiations with peak-free electron concentrations reaching as high as 2×10^{19} cm $^{-3}$. Low dose ($<10^{13}$ cm $^{-2}$) implanted donor ions were not activated by pulsed irradiations of similar range of energy densities. The reasons for this inactivity are not clear at present, and may involve several material parameters, such as concentration levels and charge states of dopants and impurities in GaAs (e.g., Cr, O, C), residual point defects or other damage, stoichiometry, and initial crystal structure through its influence on the melting temperature. More extensive studies are needed. The application of additional characterization techniques, such as deep level transient spectroscopy, photoluminescence, and electron paramagnetic resonance should prove useful.

The capability of a pulsed electron beam to directly alloy Au-Ge/Pt ohmic contacts to n-type GaAs was demonstrated. Specific contact resistance as low as 4×10^{-7} Ω -cm 2 was achieved with an electron beam pulse of appropriate energy density. To achieve good ohmic contacts, an electron beam with short pulse duration should prove more useful than conventional thermal alloying.



6.0 REFERENCES

1. K. Gamo, T. Inada, S. Krekeler, J. W. Meyer, F. H. Eisen and B. M. Welch, *Solid-State Electron* 20, 213 (1977).
2. F. H. Eisen, B. M. Welch, H. Muller, K. Gamo, T. Inada and J. M. Meyer, *Solid-State Electron* 20, 219 (1977).
3. F. H. Eisen, B. M. Welch, K. Gamo, T. Inada, H. Muller, M-A Nicolet and J. W. Meyer, *Inst. Phys. Conf. No.* 28, 64 (1976).
4. J. L. Tandon, M-A. Nicolet and F. H. Eisen, *Appl. Phys. Lett.* 34, 165 (1977).
5. S. U. Campisano, I. Catalano, G. Foti, E. Rimini, F. H. Eisen and M-A. Nicolet, *Solid-State Electron* 21, 485 (1978).
6. E. I. Shtyrkov, I. B. Khaibullin, M. M. Saripov, M. F. Galjautdinov and R. M. Bayazitov, *Sov. Phys. Semicond.* 9, 1309 (1976).
7. F. H. Eisen, J. S. Harris, B. Welch, R. D. Pashley, D. Sigund and J. M. Mayer, *Ion Implantation in Semiconductors and Other Materials*, edited by B. L. Crowder (Plenum Publishing Corp., 1973), p. 631.
8. I. V. Mitchell, J. W. Mayer, J. K. Kung and W. G. Spitzer, *J. Appl. Phys.* 42, 3982 (1971).
9. J. F. Gibbons, W. S. Johnson, S. W. Mylroie, *Projected Range Statistics*, Dowden Hutchinson and Ross, Stroudsbury, Penn. (1975).
10. S. M. Sze, *Physics of Semiconductor Devices*, Wiley-Interscience, New York, 1969, p. 40.
11. Private communication, Anton Greenwald, Spire Corporation, Bedford, MA.
12. S. S. Kular, B. J. Sealy, M. H. Badawi, K. G. Stephen, D. K. Sadana, and G. R. Booker, *Elect. Lett.* 15, 413 (1979).
13. S. U. Campisano, G. Foti, E. Rimini, F. H. Eisen, W. F. Tseng, M-A. Nicolet, and J. L. Tandon, *J. Appl. Phys.* (to be published).
14. T. N. C. Venkatesan, D. H. Auston, J. A. Golovchenko, and C. M. Surko, *AIP Conf. Proc.* 50, 629 (1979).
15. D. K. Sadana, M. C. Wilson, and G. R. Booker, *J. Microsc.* (to be published).



ERC41008.11FR

16. E. F. Kennedy, S. S. Lau, I. Golecki, J. W. Mayer, W. F. Tseng, J. A. Minnucci, and A. R. Kirkpatrick, Ref. 14, p. 470.
17. R. Tsu, J. E. Baglin, G. J. Lasher, and J. C. Tseng, Appl. Phys. Lett. 34, 153 (1979).
18. J. L. Tandon and F. H. Eisen, Ref. 14, p. 616.
19. A. M. Huber, G. Morillot, N. T. Linh, P. N. Favennec, B. Deveaud, B. Toulouse, Appl. Phys. Lett. 34, 858 (1979).
20. C. A. Evans, Jr., V. R. Deline, T. W. Sigmon, A. Lidow, Appl. Phys. Lett. 35, 291 (1979).
21. P. M. Asbeck, J. Tandon, D. Siu, R. Fairman, B. Welch, C. A. Evans, Jr., V. R. Deline, Abstract No. 14 in IEEE GaAs IC Symp., Lake Tahoe, Nevada, Sept. 1979.
22. V. L. Rideout, Solid State Electron. 18, 541 (1975).
23. H. M. Macksey, Inst. Phys. Conf. Ser. No. 33b, 254 (1977).
24. C-Y Ting, C. Y. Chen, Solid State Electron. 14, 433 (1971).
25. A. K. Sinha, T. E. Smith and H. J. Levinstein, IEEE Trans. Electron. Dev. ED-22, 218 (1975).
26. P. A. Barnes and A. Y. Cho, Appl. Phys. Lett. 33, 651 (1978).
27. T. Inada, S. Kato, T. Hara and N. Toyoda, J. Appl. Phys. 50, 4466 (1979).
28. P. A. Barnes, H. J. Leamy, J. M. Poate, S. D. Ferris, J. S. Williams and G. K. Cellar, Appl. Phys. Lett. 33, 965 (1978).
29. R. L. Mozzi, W. Fabian and F. J. Piekarski, Appl. Phys. Lett. 35, 337 (1979).
30. S. Margalik, D. Pekete, D. M. Pepper, C. P. Lee and A. Yariv, Appl. Phys. Lett. 33, 346 (1978).
31. R. B. Gold, R. A. Powell and J. F. Gibbons, Ref. 14, p. 635.
32. G. Eckhardt, C. L. Anderson, L. D. Hess and C. F. Kruman, Ref. 14, p. 641.
33. H. H. Berger, J. Electrochem. Soc.: Solid State Science and Technology 119, 507 (1972).
34. M. Witner, R. Pretorius, J. M. Mayer and M-A. Nicolet, Solid State Electron. 20, 433 (1977).



7.0 LIST OF PUBLICATIONS

- J. L. Tandon and F. H. Eisen, "Pulsed Annealing of Implanted Semi-insulating GaAs," AIP Conference Proceedings 50 (1979).
- J. L. Tandon, F. H. Eisen, I. Golecki, M-A Nicolet, D. K. Sadana, "Laser and Electron Beam Annealing of Implanted Semi-insulating GaAs," paper presented at the 37th Annual Device Research Conference, Boulder, Colorado, June 1979 (unpublished),
- I. Golecki, M. A. Nicolet, J. L. Tandon, P. M. Asbeck, D. K. Sadana, and J. Washburn, "Transient Annealing of GaAs by Electron and Laser Beams," to be published in Proceedings of the Electrochemical Society Meeting, Los Angeles, California, October 1979.
- J. L. Tandon, C. G. Kirkpatrick and F. H. Eisen, "Transient Annealing of Ion Implanted GaAs," paper presented at the 23rd SPIE Meeting, San Diego, August 1979.
- J. L. Tandon, I. Golecki, M-A Nicolet, D. K. Sadana, and J. Washburn, "Pulsed Electron Beam Induced Recrystallization and Damage in GaAs," Applied Physics Letters 35, 867 (1979)
- S. U. Campisano, G. Foti, E. Rimini, F. H. Eisen, W. F. Tseng, M-A Nicolet and J. L. Tandon, J. Appl. Phys. (to be published).
- J. L. Tandon, C. G. Kirkpatrick, B. M. Welch and P. Fleming, "Pulsed Electron Beam Alloying of Au-Ge/Pt Ohmic Contacts in GaAs," paper presented at the MRS Meeting in Boston, MA, Nov. 1979 (to be published).
- I. Golecki, M-A Nicolet, M. Mäenpää, J. L. Tandon, C. G. Kirkpatrick, D. K. Sadana, J. Wahsburn, "Transient Annealing of Implanted GaAs by a Pulsed Electron Beam," paper presented at the MRS Meeting in Boston, MA, Nov. 1979 (to be published).
- F. H. Eisen, "Laser Annealing in Compound Semi-conductors," paper presented at the MRS Meeting in Boston, MA, Nov. 1979.